Mathematisches Forschungsinstitut Oberwolfach

Report No. 1/2024

DOI: 10.4171/OWR/2024/1

Fracture as an Emergent Phenomenon

Organized by
Patrick Diehl, Baton Rouge
Robert Lipton, Baton Rouge
Anna Pandolfi, Milano
Thomas Wick, Hannover

7 January – 12 January 2024

Abstract. The mechanics of fracture propagation provides essential knowledge for the risk tolerance design of devices, structures, and vehicles. Techniques of free energy minimization provide guidance, but have limited applicability to material systems evolving away from equilibrium. Experimental evidence shows that the material response depends on driving forces arising from mechanical fields. Recent years have witnessed the development of new methods for modeling complex dynamic and quasistatic fracture. New approaches may differ remarkably from previous ones, as they involve implicit coupling between damaged and undamaged states, allowing fracture to be modeled as emergent phenomena.

The focus of this workshop is on the most advanced techniques for modeling fracture, represented by eigenerosion methods, variational approaches, phase field fracture models, and non-local approaches. Technical progress is contingent on the further development of the mathematical framework underlying these techniques. This is necessary for accurate and reliable computational modeling of fracture for multiple freely propagating cracks. The objective of this workshop is to mathematically identify and discuss open issues related to fracture modeling and to highlight recent advances. Addressing fundamental issues will foster exchange between the different communities, essential for advancing the field.

Mathematics Subject Classification (2020): 35, 49, 65, 74.

Introduction by the Organizers

The workshop *Fracture as an Emergent Phenomenon*, organized by Patrick Diehl, Robert Lipton, Anna Pandolfi and Thomas Wick, was well attended and involved 47 on site participants and 8 virtual participants with broad geographic representation from Europe and North America. The participants were a blend of researchers in Mathematics, Numerical Analysis, Scientific Computing, Materials Science, Physics, and Engineering. It included researchers investigating the free fracture problem using theoretical, numerical, and experimental tools.

In light of the diverse communities involved, the workshop consisted of three 15-minute introductory lectures given by the organizers outlining techniques used by the different communities and when applicable similarities between methodologies. These were followed by 23 forty-five-minute lectures with lively 15-minute discussions. Four shorter 15-minute lectures followed by 10 minutes of discussion were given by graduate students. The five postdoctoral researchers presented posters on their current research activity.

The workshop provided a forum and opportunity for interaction and synergy between different communities for addressing the fracture problem. Several cross-cutting issues were raised including the nucleation of fracture, homogenization of fracture, dramatic effects of elastic anisotropy on fracture paths, stability of fracture models, eigen-deformations and cohesive fracture, optimal control of fracture, experimental real-time control of fracture paths, identification of relevant length scales in fracture modeling and curvature effects in nonlocal models.

This schedule also left enough time for all participants for further discussions in smaller groups that were used with great pleasure. It turned out - according to feedback and discussions during the workshop - that indeed several people from these diverse communities would never meet at their standard conferences and explicitly stated that this has been a unique scientific occasion in which new knowledge on 'fracture' is being created.

Acknowledgement: The MFO and the workshop organizers would like to thank the National Science Foundation for supporting the participation of junior researchers in the workshop by the grant DMS-2230648, "US Junior Oberwolfach Fellows".

Workshop: Fracture as an Emergent Phenomenon

Table of Contents

Abstracts

New perspectives on non-local modeling for brittle fracture

Robert Lipton
(joint work with Debdeep Bhattacharya)

Peridynamic simulations implicitly couple the evolution of damage and deformation inside a material specimen through a nonlocal formulation using force interaction between neighboring points. They provide for the spontaneous emergence and growth of fissures as part of the dynamic simulation [6], [7]. This idea has been adapted and expanded since its inception and the literature has grown significantly since then. The time evolution of peridynamic simulations are driven by temporally and spatially nonlocal forces. What is missing so far is: 1) a complete theory for a material undergoing irreversible damage guaranteeing energy balance and 2) an explicit formula for the energy necessary for material failure and the size of a $d-1$ dimensional "fracture" set proportional to the critical energy release rate. Both of these aspects must follow directly from the evolution equation for the deformation multiplied by the velocity and integration by parts.

We rigorously pursue these aspects for the free discontinuity problem in fracture mechanics and propose a nonlocal field theory that demonstrably preserves energy balance to uncover new advantages of the nonlocal approach. Motivated by [6], the existence theory of [2], [1], [3] and the rate form of energy balance found in [4] we introduce a new nonlocal dynamic field theory to show existence of displacement-failure set pairs for two and three dimensional specimens Ω made from homogeneous material. The purpose is to model brittle damage and to recover dynamic energy balance for displacement-failure set pairs.

A small deformation model for brittle failure is constructed. Forces between pairs of points in Ω are referred to as bonds. Bond forces depend on a two-point strain. The force between pairs of points act elastically against compressive strain and for moderate tensile strain the force is linear elastic. As one continues to increase tensile strain it becomes nonlinear elastic and at a critical strain the force becomes unstable and softens with increasing strain. The force eventually goes to zero with increasing strain and the bond between points breaks. This process is irreversible and the bonds once broken do not heal. Here the maximum length scale of nonlocal interaction is both finite and small relative to the size of the domain and is denoted by ϵ. The zone of nonlocal interaction about every point is called is called the horizon. The failure set $\Gamma^\epsilon(t)$ is the set of pairs of points with broken bonds in Ω at time t.

The material is assumed to be homogeneous with density ρ and the balance of linear momentum for each point $\mathbf{x}$ in the body Ω is given by

$$\rho\ddot{\mathbf{u}}(t,\mathbf{x}) + \mathcal{L}^\epsilon[\mathbf{u}](t,\mathbf{x}) = \mathbf{b}(t,\mathbf{x}), \tag{1}$$

where $\mathbf{b}(t,\mathbf{x})$ is a prescribed body force density. The linear momentum balance is supplemented with the initial conditions on the displacement and velocity given

by

$$\mathbf{u}(0,\mathbf{x}) = \mathbf{u}_0(\mathbf{x}),\ \dot{\mathbf{u}}(0,\mathbf{x}) = \mathbf{v}_0(\mathbf{x}), \tag{2}$$

and we look for a solution $\mathbf{u}(t,\mathbf{x})$ on a time interval $0 < t < T$. The operator $\mathcal{L}^\epsilon$ is non-local both in space and time and is given by

$$\mathcal{L}^\epsilon[\mathbf{u}](t,\mathbf{x}) = -\int_\Omega \boldsymbol{f}^\epsilon(t,\mathbf{y},\mathbf{x},\mathbf{u})\, d\mathbf{y}. \tag{3}$$

Here $\boldsymbol{f}^\epsilon(t,\mathbf{y},\mathbf{x},\mathbf{u})$ is the elastic force acting on the point $\mathbf{x}$ due to the point $\mathbf{y}$ at time t due to the displacement field $\mathbf{u}$. The force is given by

$$\boldsymbol{f}^\epsilon(t,\mathbf{y},\mathbf{x},\mathbf{u}) = \frac{2\rho^\epsilon(\mathbf{y},\mathbf{x})}{\sqrt{|\mathbf{y}-\mathbf{x}|}}\gamma(\mathbf{u})(\mathbf{y},\mathbf{x},t)g'(r(t,\mathbf{u}))\boldsymbol{e}, \tag{4}$$

where $\rho^\epsilon(\mathbf{y},\mathbf{x}) = \chi_\Omega(\mathbf{y})J(|\mathbf{y}-\mathbf{x}|/\epsilon)/\omega_d\epsilon^{d+1}$, $J(|\mathbf{x}|)$ is positive and has support in the unit ball and χ_Ω is the characteristic function of the set Ω. The two point damage field $\gamma(\mathbf{u})(\mathbf{y},\mathbf{x},t)$ takes values between zero and one. Zero indicates the bond between $\mathbf{x}$ and $\mathbf{y}$ is broken and one indicates undamaged bonds, $g'(r(t,\mathbf{u}(t)))$ is the force between $\mathbf{x}$ and $\mathbf{y}$ as a function of the strain between them. The damage field $\gamma(\mathbf{u})(\mathbf{y},\mathbf{x},t)$ is nonlocal in time as well as space and depends on past values of $\mathbf{u}(t,\mathbf{x})$. This provides the coupling of damage and deformation. The operator $\mathcal{L}^\epsilon[\mathbf{u}](t,\mathbf{x})$ is the average of $\boldsymbol{f}^\epsilon(t,\mathbf{y},\mathbf{x},\mathbf{u})$ over $\mathbf{y}$ within the horizon about $\mathbf{x}$. The damage field $\gamma(\mathbf{u})(\mathbf{y},\mathbf{x},t)$ is a two point phase field. Here $\gamma(\mathbf{u})(\mathbf{y},\mathbf{x},t) = 1$ corresponds to undamaged bonds and $\gamma(\mathbf{u})(\mathbf{y},\mathbf{x},t) = 0$ corresponds to broken bonds.

This level of generalization together with Newton's second law and the new constitutive relation implicitly couple elastic forces and failure allowing failure sets and deformation to emerge from a two point strain dynamics over $\mathbb{R}^d \times \mathbb{R}^d$. In addition to existence of a solution $\mathbf{u}(t,\mathbf{x})$, the model provides energy balance. The rate form of energy balance is shown to follow directly from the evolution equation for the deformation multiplied by the velocity and integration by parts. The rate form of energy balance shows that damage must start occurring when the energy input to the system exceeds the material's ability to generate kinetic and elastic energy through displacement and velocity,. The energy expended up to time t resulting in material failure over a region $\Gamma^\epsilon(t)$ is given by a bounded $d-1$ dimensional geometric integral of the set of broken bonds given by pairs $(\mathbf{x},\mathbf{y})$ such that $\gamma(\mathbf{u})(\mathbf{y},\mathbf{x},t) = 0$ projected onto the domain Ω. Application of Gronwall's inequality shows that the geometric integral is bounded uniformly in ϵ for initial and boundary conditions that are independent of ϵ.

As an example, consider the failure set $\Gamma^\epsilon(t)$ defined by a flat two dimensional piece of surface R_t where points above the surface are no longer influenced by forces due to points below the surface and vice versa. This is the case of alignment, i.e., all bonds connecting points $\mathbf{y}$ above R_t to points $\mathbf{x}$ below are broken. Calculation of the failure energy of $\Gamma^\epsilon(t)$ shows that it is the product of the critical energy release rate of fracture mechanics multiplied by the two dimensional surface measure of R_t. The surface R_t defines an internal boundary to domain Ω and the crack

is unambiguously described as the internal boundary. Displacement jumps can only occur across R_t and traction forces are zero on either side of R_t. A similar remark can be made for one dimensional cracks inside a two dimensional body. An analysis shows that material failure is associated with a maximum energy dissipation condition on each bond.

The example given above shows that the failure energy corresponds to Griffith fracture energy for flat cracks, demonstrating that the energy is bounded and nonzero on $d-1$ dimensional sets corresponding to cracks. However the geometry of the failure set is controlled by how it grows dynamically. Growth is governed by the rate of work done against boundary forces and the dynamic interaction between elastic displacement and bond failure. Although interaction is captured implicitly through the evolution equations, one can apply the rate form of energy balance to explicitly deliver the time rate of the damage energy and characterize the location of the region undergoing damage. This region is the process zone $PZ^\epsilon(t)$ and from the constitutive law, corresponds to the regions of highest strain. The damage rate and process zone are determined by the displacement field through the rate of work done by the load and the change in both the kinetic energy and elastic potential energy of the specimen. The rate form of energy balance also dictates the onset of crack nucleation. For a flat mode-I crack in a plate the strain is greatest in a neighborhood of the tips and this the location of the process zone. Simulation using the field theory clearly show maximum strain energy dissipation as a crack path selection mechanism.

Away from the damaging zones, it is shown that the field theory delivers the energy density associated with isotropic linear elasticity. Explicit formulas for the Lamé constants in terms of the force potentials can be obtained. In this way, it is seen that the energy for this model is given by the surface energy over failure zones and a volume energy associated with linear elastic behavior inside quiescent zones. This is demonstrated for a flat crack propagating from left to right in a plate. We consider a sequence of nonlocal initial value problems for a crack propagating from left to right, parameterized by ϵ, and pass to the limit of vanishing nonlocality to find that the limit displacement field is a solution of the linear elastic wave equation outside a propagating traction free crack.

The field theory is presented in [5].

References

[1] Q. Du, Y. Tao, and X. Tian, *A peridynamic model of fracture mechanics with bond-breaking*, J. Elasticity, **132**, (2018), 197–218.

[2] E. Emmrich and D. Phust, *A short note on modeling damage in peridynamics*, J. Elasticity, **123**, (2016), 245–252.

[3] R. Lipton. *Cohesive dynamics and brittle fracture*, Journal of Elasticity, **124**, (2016), 143–191.

[4] R. Lipton, E. Said, and P. Jha, *Free damage propagation with memory*, Journal of Elasticity, **133**, (2018), 129–153.

[5] R. Lipton and D. Bhattacharya, *Energy balance and damage for brittle fracture: nonlocal formulation*, ArXiv.2401.01861v1 [mathAP] 3 Jan 2024.

[6] S. A. Silling, *Reformulation of elasticity theory for discontinuities and long-range forces*, Journal of the Mechanics and Physics of Solids, **48**, (2000), 175–209.
[7] S. A. Silling, M. Epton, O. Weckner, J. Xu, and E. Askari. *Peridynamic states and constitutive modeling*, Journal of Elasticity, **88**, (2007), 151–184.

The concept of eigenfracture and eigenerosion

Anna Pandolfi
(joint work with Kerstin Weinberg, Michael Ortiz)

According to Griffith's criterion for fracture, in a brittle material crack growth is results from the competition between elastic energy minimization and the fracture energy cost of creating new surface. Assuming rate independence, crack growth in a solid occupying a domain $\Omega \subset \mathbb{R}^3$ is governed by the potential energy

$$\Pi(u) = E(u) + (\text{forcing terms})\,, \tag{1}$$

where

$$E(u) = \int_{\Omega \setminus J_u} W(\varepsilon(u))\, dx + G_c |J_u|\,, \tag{2}$$

is the total energy, including the elastic energy of the solid and the energy cost of fracture, $W(\varepsilon(u))$ denotes the strain energy density, $\varepsilon(u) = \operatorname{sym} \nabla u$ the linearized strain tensor, $u(x)$ the displacement field, dx the element of volume and the forcing terms include body forces, boundary tractions and prescribed displacements. The jump set J_u collects the cracks across which the displacement u may jump discontinuously and $|J_u|$ denotes the crack surface area. The material-specific parameter G_c is the specific fracture energy density per unit area and measures the fracture strength of the solid.

The governing principle of energy minimization states that the displacement field u at any given time is expected to minimize the potential energy $\Pi(u)$ subject to monotonicity of the jump set J_u and to crack closure constraints. Thus, the problem of crack tracking is reduced to a pseudo-elastic problem, with monotonicity and closure constraints, for every state of loading.

The posed problem is a free-discontinuity problem in the sense that the displacement field u is allowed to be discontinuous and the jump set J_u itself is an unknown of the problem. Free-discontinuity problems are notoriously difficult to solve computationally, which has spurred the search for regularizations that relax the sharpness of the discontinuities. Here we briefly summarize three such regularizations: eigenfracture, phase-field models, and eigenerosion [1].

Eigenfracture. The method of eigenfracture (EF) is an approximation scheme for generalized Griffith models based on the notion of eigendeformation [3]. The approximating energy functional is assumed to be of the form

$$\begin{aligned} E_\epsilon(u, \varepsilon^*) &= \int_\Omega W(\varepsilon(u) - \varepsilon^*)\, dx + \frac{G_c}{2\epsilon} |\{\varepsilon^* \neq 0\}_\epsilon| \\ &= E^e(u, \varepsilon^*) + E^i_\epsilon(\varepsilon^*) \end{aligned} \tag{3}$$

where ε^* is the eigendeformation field that accounts for fracture, $E^e(u,\varepsilon^*)$ is the elastic energy, $E^i_\epsilon(\varepsilon^*)$ is the energy cost of the eigendeformation, or inelastic energy, and ϵ is a small length parameter. The elastic energy $E^e(u,\varepsilon^*)$ follows as the integral over the entire domain of the strain energy density W as a function of the total strain $\varepsilon(u)$ reduced by the eigenstrain ε^*. In this manner, eigendeformations allow the displacement field to develop jumps at no cost in elastic energy.

This local relaxation comes at the expense of a certain amount of fracture energy. The challenge in regularized models of fracture is to estimate the inelastic fracture energy $E^i_\epsilon(\varepsilon^*)$ in a manner that converges properly as $\epsilon \to 0$. In the method of eigenfracture, the crack area is estimated as the volume of the ϵ-neighborhood $\{\varepsilon^* \neq 0\}_\epsilon$ of the support $\{\varepsilon^* \neq 0\}$ of the eigendeformations scaled by $1/\epsilon$. Specifically, in this construction $\{\varepsilon^* \neq 0\}$ is the set of points where the eigendeformations differ from zero, $\{\varepsilon^* \neq 0\}_\epsilon$ is the ϵ-neighborhood of $\{\varepsilon^* \neq 0\}$, i. e., the set of points at a distance to $\{\varepsilon^* \neq 0\}$ less or equal to ϵ, and $|\{\varepsilon^* \neq 0\}_\epsilon|$ is the volume of $\{\varepsilon^* \neq 0\}_\epsilon$.

The method of eigenfracture is provably convergent [3], in the sense that the total energy (3) Γ-converges to the Griffith energy (2) in the limit of $\epsilon \to 0$. This convergence property shows that the eigenfracture method is indeed physically and mathematically sound.

Phase-field models of fracture. In the PF approximation of Griffith fracture, the state of the material is characterized by an additional continuous field $v(x)$ taking values in the interval $[0,1]$ and $v = 0$ at the crack. The crack set J_u is then approximated as a diffuse interface where $v \neq 1$. The corresponding fracture model traces back to the pioneering work of Ambrosio and Tortorelli [4], who showed that a two-field functional Γ-converges to the Mumford-Shah functional of image segmentation. Generalized to three-dimensional elasticity, the two-field functional of Ambrosio and Tortorelli assumes the form

$$\begin{aligned} E_\epsilon(u,v) &= \int_\Omega \Big((v^2 + o(\epsilon)) W(\varepsilon(u)) + G_c \Big(\frac{(1-v)^2}{4\epsilon} + \epsilon |\nabla v|^2 \Big) \Big)\, dx \\ &= E^e_\epsilon(u,v) + E^i_\epsilon(v), \end{aligned} \tag{4}$$

where ϵ is a small length parameter and $o(\epsilon)$ stands in for a positive function that decreases to zero faster than the small parameter ϵ. The work of Ambrosio and Tortorelli, and other similar works [5, 2], subsequently spawned numerous variants, extensions and implementations, but the differential structure of the fracture energy $E^i_\epsilon(v)$ in (4) has remained essentially unchanged in the later works.

Eigenerosion. Eigenerosion (EE) supplies an efficient implementation of the eigenfracture model [6]. To establish the connection between eigenfracture, eq. (3), and eigenerosion, assume that $W(\varepsilon)$ is quadratic and restrict eigendeformations to the particular form

$$\varepsilon^* = \varepsilon(u) - (w + o(\epsilon))^{1/2} \varepsilon(u), \tag{5}$$

with w taking the values 0 or 1, i. e., $w(x) \in \{0, 1\}$. Inserted into eq. (3) this gives the EE functional

$$E_\epsilon(u, w) = \int_\Omega (w + o(\epsilon))W(\varepsilon(u))\, dx + \frac{G_c}{2\epsilon}|\{w = 0\}_\epsilon| = E^e_\epsilon(u, w) + E^i_\epsilon(w). \tag{6}$$

By Jensen's inequality and properties of extreme points [7], it follows that the range of w can be extended to the entire interval $[0, 1]$, i. e., $0 \leq w(x) \leq 1$, without changing the solutions. Thus, EE is a restricted form of eigenfracture and it supplies an upper bound of the eigenfracture energy in general.

Evidently, the EE energy (6) may be regarded as a PF model with phase field

$$v = \sqrt{w} \tag{7}$$

and a fracture energy computed by the ϵ-neighborhood construction. Conversely, PF models of fracture may be viewed as special cases of EE, and hence eigenfracture, where the fracture energy is of the Ambrosio-Tortorelli type.

The great advantage of the EE model (6) *vs.* the conventional Ambrosio–Tortorelli–type phase-field model (4) is that in the former, eq. (6), the phase-field is undifferentiated and evaluates the fracture energy through an integral expression, whereas the latter, eq. (4), requires the phase-field to be differentiated. Differentiation in turn requires regularity and conforming interpolation, e. g., by the finite-element method. By contrast, the integral form of the fracture energy in (6) allows the phase-field to be approximated, e. g., as piecewise constant 0 or 1, which leads to a considerable increase in implementational simplicity and robustness [6, 8].

References

[1] A. Pandolfi, K. Weinberg, and M. Ortiz. *A comparative accuracy and convergence study of eigenerosion and phase-field models of fracture. Computer Methods in Applied Mechanics and Engineering*, 386:114078, 2021.

[2] L. Ambrosio, N. Fusco, and D. Pallara. *Functions of Bounded Variation and Free Discontinuity Problems*. Oxford University Press, Oxford – New York, 2000.

[3] B. Schmidt, F. Fraternali, and M. Ortiz. Eigenfracture: an eigendeformation approach to variational fracture. *SIAM Multiscale Modeling & Simulation*, 7(3):1237–1266, 2009.

[4] L. Ambrosio and V. M. Tortorelli. On the approximation of free discontinuity problems. *Bollettino dell'Unione Matematica Italiana 6-B*, 7:105–123, 1992.

[5] A. Braides and G. Dal Maso. Nonlocal approximation of the Mumford-Shah functional. *Calculus of Variations and Partial Differential Equations*, 5:293–322, 1997.

[6] A. Pandolfi and M. Ortiz. An eigenerosion approach to brittle fracture. *International Journal for Numerical Methods in Engineering*, 92(8):694–714, 2012.

[7] C. J. Larsen. Local minimality and crack prediction in quasi-static griffith fracture evolution. *Discrete & Continuous Dynamical Systems-S*, 6(1):121, 2013.

[8] A. Pandolfi, B. Li, and M. Ortiz. Modeling fracture by material-point erosion. *International Journal of Fracture*, 184(1-2):3–16, 2013.

Brief introduction to variational / phase-field fracture

Thomas Wick

This short talk serves to give a brief introduction and overview of variational / phase-field method for modeling fracture to the audience of this workshop. As this workshop is composed by three groups of people, namely peridynamics, eigenerosion, phase-field, as well as experimentalists, scientific computing, numerical analysis, and theoretical mathematics, the principle properties of phase-field fracture shall be explained in order to enable a common starting point for fruitful discussions. A corresponding overview paper addressing mainly peridynamics and phase-field, but with literature references to eigenerosion as well, is [4].

In phase-field fracture, the principal idea (here explained for quasi-static fracture in brittle materials) is based on energy minimization in which potential and fracture energies interact [2]. To this end, let $\Omega \subset \mathbb{R}^n$ be the intact domain and $\Gamma \subset \mathbb{R}^{n-1}$ the fracture set. Let $\mathbf{u} : \Omega \to \mathbb{R}^n$ be a displacement field and the total energy be given by

$$E(\mathbf{u}, \Gamma) = \underbrace{\int_\Omega \psi_0(\epsilon(\mathbf{u}))dV - F(\mathbf{u})}_{=:P(\mathbf{u})} + \underbrace{\int_\Gamma G_c \, dA}_{=\psi_c(\Gamma)},$$

with the potential energy

$$P(\mathbf{u}) := \int_\Omega \psi_0(\epsilon(\mathbf{u}))dV - F(\mathbf{u}),$$

composed by the bulk energy (first term) with $\psi_0(\epsilon(\mathbf{u})) := \mathrm{C}\epsilon(\mathbf{u}) \cdot \epsilon(\mathbf{u})$ being the energy storage function with the stiffness tensor $\mathrm{C} \in \mathbb{R}^{n\times n\times n\times n}$, and the linearized strain tensor $\epsilon(\mathbf{u}) = \frac{1}{2}(\nabla\mathbf{u} + \nabla\mathbf{u}^T)$. The external potential of volume and surface forces is given by

$$F(\mathbf{u}) = \int_\Omega \mathbf{b}^*\mathbf{u}dV + \int_{\partial\Omega_t} \mathbf{t}^*\mathbf{u}dA, \tag{1}$$

where $\mathbf{b}^*$ is the distributed body force and $\mathbf{t}^*$ are traction forces. The crack surface energy is given by

$$\psi_c(\Gamma) = \int_\Gamma G_c \, dA, \tag{2}$$

where $G_c > 0$ is the critical energy release rate. The domain Ω describes the solid with a (sharp) crack set Γ. For the boundary $\partial\Omega$ of the domain Ω two kinds of boundary conditions along the normal vector $\mathbf{n}$ are considered such that $\partial\Omega_u \cap \partial\Omega_t = \emptyset$. On the boundary $\partial\Omega_u$ Dirichlet displacement conditions are applied, which are built, as usually done, into the governing function spaces. Tractions $\mathbf{t}^*$ are applied to the $\partial\Omega_t$ boundary.

From mathematical and numerical viewpoints, the sharp fracture representation (2) is challenging because the crack 'lives' on a lower-dimensional manifold Γ.

On the one hand, this requires special function spaces, e.g., SBV spaces, and on the other hand, numerical approximations require specialized discretizations as for instance generalized/extended finite elements among various other possible techniques.

To handle this challenge one can borrow techniques from image processing. The single-well Modica-Mortola functional is introduced by Ambrosio and Tortorelli [1] in image processing to approximate the the surface area term in the Mumford–Shah functional and is given by

$$\int_{\Gamma} dA \approx \int_{\Omega_c} \gamma(\phi, \nabla\phi) dV, \tag{3}$$

with

$$\gamma(\phi, \nabla\phi) = \frac{1}{2}\left[\frac{1}{l_0}(1-\phi)^2 + l_0|\nabla\phi|^2\right]. \tag{4}$$

Bourdin et al. [3] proposed to use this energy in an appealing approach to regularize the sharp crack defined on Γ by a domain integral defined on Ω_c. In this context it is given by

$$\int_{\Gamma} G_c dA \approx \int_{\Omega_c} G_c \gamma(\phi, \nabla\phi) dV, \tag{5}$$

with $\gamma(\phi, \nabla\phi)$ is now viewed physically as the crack surface density function. Here, $l_0 > 0$ is the so-called length scale (i.e., regularization) parameter and l_0 characterizes the width of the regularized domain Ω_c.

Based on these ingredients phase-field modeling has seen world-wide developments with extensions in all directions such as other constitutive stress tensors and their splitting into tension and compressive forces, multiphysics extensions into porous media and thermo-elasticity, improvements of algorithms for nonlinear and linear solvers, goal functional (quantities of interest) evaluations, optimization loops, parameter identification, up to data-driven approaches, to name a few. All these developments pose new questions and discussions from which some of them shall be discussed during this workshop.

References

[1] L. Ambrosio and V.M. Tortorelli, *Approximation of functionals depending on jumps by elliptic functionals via* Γ*-convergence*, Comm. Pure Appl. Math., **43**, pp. 999–1036, 1990

[2] G.A. Francfort and J.-J. Marigo, *Revisiting brittle fracture as an energy minimization problem*, J. Mech. Phys. Solids, **46**(8), pp. 1319–1342, 1998

[3] B. Bourdin and G.A. Francfort and J.-J. Marigo, *Numerical experiments in revisited brittle fracture*, J. Mech. Phys. Solids, **48**(4), 797–826, 2000

[4] P. Diehl, R. Lipton, T. Wick, M. Tyagi, *A comparative review of peridynamics and phase-field models for engineering fracture mechanics*, Comput. Mech. **69**, 1259–1293 (2022).

[5] T. Wick, *Multiphysics Phase-Field Fracture: Modeling, Adaptive Discretizations, and Solvers*, Radon Series on Computational and Applied Mathematics, **Band 28**, de Gruyter, October 2020

Homogenisation of free discontinuity problems

Gianni Dal Maso

Free discontinuity problems are minimum problems for functionals of the form

$$\int_{A\setminus J_u} f(x,\nabla u)dx + \int_{A\cap J_u} g(x,[u],\nu_u)d\mathcal{H}^{d-1}, \tag{1}$$

where $A \subset \mathbb{R}^d$ is a given open set, J_u is the jump set of u (assumed to be a $(d-1)$-dimensional set), $[u] = u^+ - u^-$ is the amplitude of the jump of u, ν_u is the unit normal to J_u, and $\mathcal{H}^{d-1}$ is the $(d-1)$-dimensional Hausdorff measure.

In the applications to *fracture mechanics* u represents the *displacement* and its jump set J_u is interpreted as the *crack* (for simplicity we consider here only the *antiplane case*, where the displacement is a scalar function), and (1) represents the sum of the stored elastic energy and of the energy dissipated by the crack.

In *brittle* fracture models we assume $\inf g > 0$; typical example $g(x,\zeta,\nu) = 1$.

In the *cohesive* models we assume $g(x,0,\nu) = 0$ and the existence of the limit $\lim_{t\to 0+} \frac{1}{t} g(x,t\zeta,\nu) =: g^0(x,\zeta,\nu) < +\infty$; typical example $g(x,\zeta,\nu) = |\zeta| \wedge 1$. This condition reflects a *force acting between the crack lips* when the opening is small.

In both cases we assume that g is *bounded*. This is due to the fact that *no force is acting between the crack lips* when the crack opening is sufficiently large.

Free discontinuity problems are studied in function spaces containing functions that may be discontinuous across a $(d-1)$-dimensional surface, like $BV(A)$. For every $u \in BV(A)$ the gradient Du of u in the sense of distributions is a bounded Radon measure that can be decomposed as $Du = D^a u + D^s u = D^a u + D^j u + D^c u$, where $D^a u$ is *absolutely continuous* with respect to the Lebesgue measure (its density is denoted by ∇u), $D^s u$ is *singular*, $D^j u$ (the *jump part*) is the restriction of $D^s u$ to the jump set, and $D^c u$ (the *Cantor part*) is the remaining part of $D^s u$.

In the *brittle* case, when $\inf g > 0$, it is convenient to formulate these problems in the space $SBV(A)$ of *special functions of bounded variation*, introduced by Ambrosio and De Giorgi in [7] and defined as the space of all $u \in BV(A)$ such that $D^c u = 0$. Under suitable technical assumptions that ensure the lower semicontinuity of the functional, it is possible to prove the existence of a solution of the free discontinuity problem by using a *compactness* result for $SBV(A)$ due to Ambrosio [1, 2].

In the *cohesive* case the compactness result in $SBV(A)$ cannot be applied. Moreover the functional (1) is *not lower semicontinuous* in $BV(A)$ and one has to consider its relaxed version, which, under suitable hypotheses, can be written as

$$\int_A f(x,\nabla u)dx + \int_A f^\infty(x,\frac{dD^c u}{d|D^c u|})d|D^c u| + \int_{A\cap J_u} g(x,[u],\nu_u)d\mathcal{H}^{d-1},$$

where $\frac{dD^c u}{d|D^c u|}$ is the Radon-Nikodym derivative of the measure $D^c u$ with respect to its variation $|D^c u|$ and $f^\infty(x,\xi) := \limsup_{t\to+\infty} \frac{1}{t} f(x,t\xi)$ is the recession function. Unfortunately this functional does not control the BV-norm of u, since it does not control the amplitude of the jump $[u]$. Recall that g is bounded, so we cannot have $c|[u]| \le g(x,[u],\nu_u)$.

Therefore, we formulate the problem in the larger space $GBV_\star(A)$, defined as the space of functions $u\colon A \to \mathbb{R}$ whose truncations $u^{(m)} := (u \wedge m) \vee (-m)$ belong to $BV(A)$ for every $m > 0$ and satisfy

$$\sup_{m>0} \Big(\int_A |\nabla u^{(m)}| dx + |D^c u^{(m)}|(A) + \int_{J_{u^{(m)}}} |[u^{(m)}]| \wedge 1 d\mathcal{H}^{d-1} \Big) < +\infty \,.$$

The main point is that, although Du is not defined (u might not be a distribution!), $D^c u$ can be defined for every $u \in GBV_\star(A)$ (see [5]).

The *homogenization* problem for free discontinuity functionals leads to the study of the asymptotic behaviour, as $\varepsilon \to 0+$, of the minimisers of the functionals

$$\int_A f(\frac{x}{\varepsilon}, \nabla u) dx + \int_{A \cap J_u} g(\frac{x}{\varepsilon}, [u], \nu_u) d\mathcal{H}^{d-1}, \tag{2}$$

$$\int_A f(\frac{x}{\varepsilon}, \nabla u) dx + \int_A f^\infty(\frac{x}{\varepsilon}, \frac{dD^c u}{d|D^c u|}) d|D^c u| + \int_{A \cap J_u} g(\frac{x}{\varepsilon}, [u], \nu_u) d\mathcal{H}^{d-1}, \tag{3}$$

in the *brittle* and *cohesive* cases, respectively. For this we use Γ-convergence.

In the *brittle* case f has p-growth, i.e., $a_1|\xi|^p \le f(x,\xi) \le a_2(|\xi|^p + 1)$ for some constants $p > 1$ and $0 < a_1 \le a_2$, while $0 < c_1 \le g(x, \zeta, \nu) \le c_2$ for some constants $0 < c_1 \le c_2$. We use the following notation:

- $Q(x,\rho)$ = cube with centre x and side ρ, with faces parallel to the axes;
- $Q_\nu(x,\rho)$ = cube with centre x and side ρ, with a face orthogonal to ν;
- ℓ_ξ = linear function with gradient ξ, i.e., $\ell_\xi(x) = \xi \cdot x$;
- $u_{x,\zeta,\nu}$ = pure jump function defined by $u_{x,\zeta,\nu}(y) = \zeta$ if $(y-x)\cdot\nu > 0$ and $u_{x,\zeta,\nu}(y) = 0$ if $(y-x)\cdot\nu \le 0$;
- $m^{1,p}(\ell_\xi, Q(x,\rho)) := \inf\{\int_{Q(x,\rho)} f(y, \nabla u) dy : u - \ell_\xi \in W^{1,p}_0(Q(x,\rho))$;
- $m^{pc}(u_{x,\zeta,\nu}, Q_\nu(x,\rho)) := \inf\{\int_{Q_\nu(x,\rho)\cap J_v} g(y,[u],\nu_u) d\mathcal{H}^{d-1} : u$ piecewise constant on $Q_\nu(x,\rho)$, $u = u_{x,\zeta,\nu}$ on $\partial Q_\nu(x,\rho)\}$.

Theorem 1 (see [3]). *In the* brittle *case assume that the limits*

$$\lim_{\rho\to+\infty} \frac{m^{1,p}(\ell_\xi, Q(\rho x,\rho))}{\rho^d} =: f_{hom}(\xi) \tag{4}$$

$$\lim_{\rho\to+\infty} \frac{m^{pc}(u_{\rho x,\zeta,\nu}, Q_\nu(\rho x,\rho))}{\rho^{d-1}} =: g_{hom}(\zeta,\nu) \tag{5}$$

exist and are independent of x. *Then the functionals*

$$\int_A f(\frac{x}{\varepsilon}, \nabla u) dx + \int_{A\cap J_u} g(\frac{x}{\varepsilon}, [u], \nu_u) d\mathcal{H}^{d-1},$$

which are well defined on the space $GSBV(A)$ of functions whose truncations belong to $SBV(A)$, Γ-converge, as $\varepsilon \to 0+$, to the functional

$$\int_A f_{hom}(\nabla u) dx + \int_{A\cap J_u} g_{hom}([u], \nu_u) d\mathcal{H}^{d-1}.$$

In [4] a stochastic homogenisation result for free discontinuity problems in the *brittle* case has been obtained. It shows that (4) and (5) are almost surely satisfied under the natural hypotheses for stochastic homogenisation.

In the *cohesive* case f has *linear growth*, i.e., $a_1|\xi| \le f(x,\xi) \le a_2(|\xi|+1)$ for some constants $0 < a_1 \le a_2$, $c_1(|\zeta| \wedge 1) \le g(x,\zeta,\nu) \le c_2(|\zeta| \wedge 1)$ for some constants $0 < c_1 \le c_2$, and the limit $g^0(x,\zeta,\nu) := \lim_{t\to 0+} \frac{1}{t} g(x,t\zeta,\nu)$ exists and is finite. Given a bounded open set $A \subset \mathbb{R}^d$ with Lipschitz boundary, we define

$$E^{f,g}(u,A) := \int_A f(x,\nabla u)dx + \int_A f^\infty(x, \frac{dD^c u}{d|D^c u|})d|D^c u| + \int_{A\cap J_u} g(x,[u],\nu_u)d\mathcal{H}^{d-1};$$

similar definitions for $E^{f,g^0}(u,A)$ and $E^{f^\infty,g}(u,A)$. For every $t > 0$ we define

$$m_t^{f,g^0}(\ell_\xi, A) := \inf\{E^{f,g^0}(u,A) : u \in BV(A),\ |u-\ell_\xi| \le t,\ u = \ell_\xi \text{ on } \partial A\}$$
$$m^{f^\infty,g}(u_{x,\zeta,\nu}, A) := \inf\{E^{f^\infty,g}(u,A) : u \in BV(A),\ u = u_{x,\zeta,\nu} \text{ on } \partial A\}.$$

Theorem 2 (see [6]). *In the* cohesive *case for every $\xi \in \mathbb{R}^d$ there exists an explicit constant $\kappa_\xi > 0$ such that, if the limits*

$$\lim_{\rho\to+\infty} \frac{m_{\kappa_\xi\rho}^{f,g^0}(\ell_\xi, Q(\rho x,\rho))}{\rho^d} =: f_{hom}(\xi) \tag{6}$$

$$\lim_{\rho\to+\infty} \frac{m^{f^\infty,g}(u_{\rho x,\zeta,\nu}, Q_\nu(\rho x,\rho))}{\rho^{d-1}} =: g_{hom}(\zeta,\nu) \tag{7}$$

exist and are independent of x, *then the functionals*

$$\int_A f(\frac{x}{\varepsilon},\nabla u)dx + \int_A f^\infty(\frac{x}{\varepsilon}, \frac{dD^c u}{d|D^c u|})d|D^c u| + \int_{A\cap J_u} g(\frac{x}{\varepsilon},[u],\nu_u)d\mathcal{H}^{d-1},$$

defined on $GBV_\star(A)$, Γ-converge, as $\varepsilon \to 0+$, to the functional

$$\int_A f_{hom}(\nabla u)dx + \int_A f_{hom}^\infty(\frac{dD^c u}{d|D^c u|})d|D^c u| + \int_{A\cap J_u} g_{hom}([u],\nu_u)d\mathcal{H}^{d-1}.$$

Using the technique developed in [4], from this theorem one can obtain a stochastic homogenisation result for free discontinuity problems in the *cohesive* case, which shows that (6) and (7) are almost surely satisfied.

References

[1] L. Ambrosio, *A compactness theorem for a new class of functions of bounded variation.* Boll. Un. Mat. Ital. B (7) **3** (1989), 857–881.

[2] L. Ambrosio, *Existence theory for a new class of variational problems.* Arch. Rational Mech. Anal. **111** (1990), 291–322.

[3] F. Cagnetti, G. Dal Maso, L. Scardia, C.I. Zeppieri, *Γ-convergence of free-discontinuity problems.* Ann. Inst. H. Poincaré C Anal. Non Linéaire **36** (2019), 1035–1079.

[4] F. Cagnetti, G. Dal Maso, L. Scardia, C.I. Zeppieri, *Stochastic homogenisation of free-discontinuity problems.* Arch. Ration. Mech. Anal. **233** (2019), 935–974.

[5] G. Dal Maso, R. Toader, *A new space of generalised functions with bounded variation motivated by fracture mechanics.* NoDEA Nonlinear Differential Equations Appl. **29** (2022), Paper No. 63.

[6] G. Dal Maso, R. Toader, *Homogenisation problems for free discontinuity functionals with bounded cohesive surface terms.* Preprint SISSA, Trieste, 2023.
[7] E. De Giorgi, L. Ambrosio, *New functionals in the calculus of variations. (Italian)* Atti Accad. Naz. Lincei Rend. Cl. Sci. Fis. Mat. Nat. (8) **82** (1988), 199–210.

Identification of damage from 4D displacement field measurements

Ana Vrgoc (PhD student talk)

Digital Volume Correlation (DVC) approaches enable quantitative analyses of specimen deformations to be performed by measuring 3D displacement fields between discrete states of samples imaged via, say, X-Ray Computed Tomography. Such frameworks are limited by the number of scans (due to acquisition duration). Considering only one projection per loading step, Projection-based Digital Volume Correlation (P-DVC) allows 4D (i.e., space and time) full- field measurements to be carried out over entire loading histories. The sought displacement field is generally decomposed over a basis of separated variables, namely, temporal and spatial modes. In the present work, the spatial modes are constructed via scan-wise DVC and only the temporal amplitudes are sought via P-DVC. The proposed method is applied to a specimen subjected to in-situ tension (i.e., imaged via X-Ray Computed Tomography). The P-DVC enhanced DVC method employed herein enables for the quantification of damage growth over the entire loading history up to failure.

Analysis and simulation of a rate-independent phase-field damage model

Dorothee Knees
(joint work with Samira Boddin, Felix Rörentrop, Jörn Mosler)

We focus here on a phase-field model first introduced by Ambrosio and Tortorelli as a diffuse approximation of sharp fracture models. For this model, the underlying energy is not simultaneously convex in all variables. In rate-independent models this causes problems since there might be no time-continuous solutions even if the applied loads are varying smoothly with time. Different (weak) solution concepts were developed that allow for discontinuous solutions, see [11] for an overview. In general nonconvex cases, they typically are not equivalent. As a consequence, different solution concepts might predict different critical loads at which failure occurs. Hence, it is desirable to understand which of these concepts is most appropriate from the physical point of view and to clarify which numerical schemes should be used to approximate solutions of a certain class.

A meanwhile well established solution concept is that of *(Global) Energetic Solutions*, first introduced in [12] and applied to damage models in [13, 10, 3]. It relies on a global minimization principle. However, from a physics point of view, due to the global minimization such solutions tend to jump too early. For instance, this means that solutions develop a discontinuity even though local force

balances would predict no evolution at all, see [8] for an example with a single propagating crack. To avoid this problem the class of *Balanced Viscosity Solutions* (BV solutions) was introduced, see for instance [9] for the general theory and [6, 7] for its application to damage and phase-field fracture models. Here, a viscosity term/damping term is introduced into the model and the viscous limit (i.e. vanishing viscosity parameter) is investigated. In this way, a solution class is introduced that appears to have more realistic jump conditions compared to the gobal energetic approach. In this note we focus on balanced viscosity solutions for the Ambrosio-Tortorelli model and describe a time-adaptive algorithm that can be applied to approximate such solutions, [1].

Let us first describe the model and our assumptions. Let $\Omega \subset \mathbb{R}^2$ be a bounded domain with Lipschitz boundary. Let $u : [0,T] \times \Omega \to \mathbb{R}^2$ with $u(t) \in \mathcal{U} := H^1_0(\Omega, \mathbb{R}^2)$ denote the displacement field and $z : [0,T] \times \Omega \to \mathbb{R}$ with $z(t) \in H^1(\Omega) =: \mathcal{Z}$ denote the scalar damage variable. Here, $z(x) = 1$ means no damage in $x \in \Omega$ while $z(x) = 0$ means maximum damage in x. Given a load $\ell \in \mathrm{C}^{1,1}([0,T];\mathcal{U}^*)$ the stored energy functional reads for $u \in \mathcal{U}$ and $z \in \mathcal{Z}$

$$\mathcal{E}(t,u,z) = \tfrac{1}{2}\int_\Omega g(z)\mathbb{C}e(u) : e(u)\,\mathrm{d}x + \tfrac{1}{2}\int_\Omega \kappa_1 z^2 + \kappa_2|\nabla z|^2\,\mathrm{d}x - \langle \ell(t), u\rangle, \tag{1}$$

where $e(u) = \mathrm{sym}\nabla u$ is the symmetrized strain and κ_1, κ_2 are some positive constants. Moreover, $g(z) = (z^2 + \eta)$ for some $\eta > 0$. For $v \in \mathcal{Z}$ and fixed $\mu > 0$, the dissipation potential is given by

$$\mathcal{R}(v) = \begin{cases} \int_\Omega \mu v\,\mathrm{d}x & \text{if } v \le 0 \\ \infty & \text{otherwise} \end{cases}.$$

The quasistatic evolution model written as a force balance reads: Given $z_0 \in \mathcal{Z}$ determine u and z such that $z(0) = z_0$ and for $t \in [0,T]$

$$0 = \mathrm{D}_u\mathcal{E}(t,u(t),z(t)), \tag{2}$$

$$0 \in \partial\mathcal{R}(\dot z(t)) + \mathrm{D}_z\mathcal{E}(t,u(t),z(t))\,. \tag{3}$$

In order to prove the existence of solutions via a vanishing viscosity procedure, the differential inclusion (3) is regularized by adding the term $\nu\dot z(t)$ with a positive parameter ν. Solutions (u_ν, z_ν) of the regularized system do exist and are continuous in time. In [6], the vanishing viscosity analysis for $\nu \to 0$ is carried out. For that purpose an arc-length parameterization for the solution trajectories was introduced. Let $\mathcal{I}(t,z) = \min\{\mathcal{E}(t,v,z)\,;\, v \in \mathcal{U}\}$ denote the reduced energy functional. It is shown that in the parameterized setting the limits $\nu \to 0$ of the sequences (u_ν, z_ν) can be characterized as follows:

Theorem 1. *Assume that* $\mathrm{D}_z\mathcal{I}(0,z_0) \in L^2(\Omega)$. *There exists* $S > 0$ *and functions* $\hat t \in W^{1,\infty}([0,S],[0,T])$ *and* $\hat z \in W^{1,\infty}((0,S);\mathcal{Z})$ *with* $\hat z(0) = z_0$ *satisfying for almost all* $s \in [0,S]$ *the normalization condition* $\hat t'(s) + \|\hat z'(s)\|_{\mathcal{Z}} \le 1$ *and the*

energy dissipation balance

$$\mathcal{I}(\hat{t}(s),\hat{z}(s)) + \int_0^s \mathcal{R}(\hat{z}'(r)) + \mathcal{D}_{\partial\mathcal{R}(0)}(\hat{t}',\hat{z}',-\mathrm{D}_z\mathcal{I}(\hat{t},\hat{z}))\,\mathrm{d}r \\ = \mathcal{I}(0,z_0)) + \int_0^s \hat{t}'(r)\partial_t\mathcal{I}(\hat{t}(r),\hat{z}(r))\,\mathrm{d}r,$$

where

$$\mathcal{D}_{\partial\mathcal{R}_1(0)}(\hat{t}',\hat{z}',\xi) = \begin{cases} \operatorname{dist}(\xi,\partial\mathcal{R}(0))\,\|\hat{z}'\|_{L^2(\Omega)} & \text{if } \hat{t}'=0 \\ \chi_{\{0\}}(\operatorname{dist}(\xi,\partial\mathcal{R}(0))) & \text{if } \hat{t}'>0 \end{cases}.$$

This is also the definition of ($\mathcal{Z}$-parameterized) balanced viscosity solutions in this context. One could now apply a time-incremental version of the vanishing viscosity procedure to approximate balanced viscosity solutions numerically. The convergence of solutions of such schemes to balanced viscosity solutions was analyzed in [6], as well. However, the numerical experiments in [8] (that were carried out for the propagation of a single crack) showed that it is very difficult to choose the time increment and the viscosity parameter in a good way so that already for coarse discretizations the correct behavior is visible.

An alternative way to approximate balanced viscosity solutions is based on a procedure suggested in [2]: Instead of discretizing the time one discretizes with respect to the arc-length parameter of the solution trajectories. In [1], we combined this approach with an alternate minimization scheme and analyzed the following time-adaptive local minimization algorithm: Let $\rho>0$ denote a locality parameter and let $\mathcal{V}=L^\alpha(\Omega)$, $\alpha\geq\frac{3p}{p-2}$, or $\mathcal{V}=H^1(\Omega)$. Here, $p>2$ is given by a theorem about the uniform higher integrability of the strains ([4, 1]). In general, this value unfortunately is not known explicitly.

The scheme reads: Given (t_k,u_k,z_k) determine the values $(t_{k+1},u_{k+1},z_{k+1})$ by

- inner loop: constrained alternate minimization, $i\in\mathbb{N}_0$

$$u_{k,i} = \operatorname{argmin}\{\,\mathcal{E}(t_k,v,z_{k,i-1})\,;\,v\in\mathcal{U}\,\} \tag{4}$$

$$z_{k,i} = \operatorname{argmin}\{\,\mathcal{E}(t_k,u_{k,i},\zeta)+\mathcal{R}(\zeta-z_k)\,;\,\zeta\in\mathcal{Z},\,\|\zeta-z_{k,i-1}\|_{\mathcal{V}}\leq\rho\,\} \tag{5}$$

  There exist subsequences with

$$u_{k+1} := \lim_{m\to\infty} u_{k,i_m} \text{ strongly in } \mathcal{U},\ z_{k+1} := \lim_{m\to\infty} z_{k,i_m} \text{ strongly in } \mathcal{Z}.$$

  The limits are fixed points of (4)–(5).
- outer loop/time update: $t_{k+1} := t_k + \rho - \|z_{k+1}-z_k\|_{\mathcal{V}}$.
- Repeat until $t_{k+1}=T$.

The following convergence result is proved in [1]:

Theorem 2. *Let $z_0\in\mathcal{Z}$, $0\leq z_0\leq 1$ and $\widetilde{u}_0\in\mathcal{U}$ such that $\mathrm{D}_z\mathcal{E}(0,\widetilde{u},z_0)\in\mathcal{V}^*$. Then there exists a sequence $\rho_n\to 0$, $S>T$ and functions*

$$\hat{t}\in W^{1,\infty}(0,S;\mathbb{R}),\qquad \hat{u}\in W^{1,\infty}(0,S;W^{1,\widetilde{p}}(\Omega)),$$
$$\hat{z}\in W^{1,\infty}(0,S;\mathcal{V})\cap L^\infty(0,S;\mathcal{Z})\cap H^1(0,S;\mathcal{Z})$$

such that suitable interpolants converge weakly in the above spaces. Moreover, the limit functions form a $\mathcal{V}$-parameterized BV-solution:*

- *Complementarity: For a.a. $s \in [0,S]$:*

$$\hat{t}'(s) \geq 0, \quad \hat{t}'(s) + \left\|\hat{z}'(s)\right\|_{\mathcal{V}} \leq 1$$
$$\hat{t}'(s)\,\mathrm{dist}_{\mathcal{V}^*}\left(-\mathrm{D}\mathcal{E}(\hat{t}(s),\hat{u}(s),\hat{z}(s)), \partial^{\mathcal{Z}}\mathcal{R}(0)\right) = 0\,.$$

- *Balance of linear momentum:* $\mathrm{D}_u\mathcal{E}(\hat{t}(s),\hat{u}(s),\hat{z}(s)) = 0 \quad$ *in* $\mathcal{U}^*$.
- *Energy disspation balance: for all s*

$$\mathcal{E}(\hat{t}(s),\hat{u}(s),\hat{z}(s)) + \int_0^s \mathcal{R}(\hat{z}') + \left\|\hat{z}'\right\|_{\mathcal{V}} \mathrm{dist}_{\mathcal{V}}(-\mathrm{D}_z\mathcal{E}(\hat{t},\hat{u},\hat{z}), \partial^{\mathcal{Z}}\mathcal{R}(0))\mathrm{d}\sigma$$
$$= \mathcal{E}(0,u_0,z_0) + \int_0^s \partial_t\mathcal{E}(\hat{t},\hat{u},\hat{z})\hat{t}'\mathrm{d}\sigma\,.$$

Numerical examples in [1] demonstrate the behavior of the algorithm.

In [5], we analyzed a time-incremental alternate minimization algorithm. There, we also identified the limit as the time step size tends to zero. The numerical examples from [1] suggest that there is no difference in the solutions provided by the local minimization scheme combined with alternate minimization and the pure alternate minimization scheme. However, first finite dimensional examples show that solutions obtained via a pure alternate minimization procedure do not necessarily belong to the class of balanced viscosity solutions.

References

[1] S. Boddin, F. Rörentrop, D. Knees, and J. Mosler. Approximation of balanced viscosity solutions of a rate-independent damage model by combining alternate minimization with a local minimization algorithm, 2022. arXiv, 2211.12940.

[2] M. A. Efendiev and A. Mielke. On the rate-independent limit of systems with dry friction and small viscosity. *J. Convex Anal.*, 13(1):151–167, 2006.

[3] A. Giacomini. Ambrosio-Tortorelli approximation of quasi-static evolution of brittle fractures. *Calc. Var. Partial Differential Equations*, 22(2):129–172, 2005.

[4] R. Herzog, C. Meyer, and G. Wachsmuth. Integrability of displacement and stresses in linear and nonlinear elasticity with mixed boundary conditions. *J. Math. Anal. Appl.*, 382(2):802–813, 2011.

[5] D. Knees and M. Negri. Convergence of alternate minimization schemes for phase-field fracture and damage. *Math. Models Methods Appl. Sci.*, 27(9):1743–1794, 2017.

[6] D. Knees, R. Rossi, and C. Zanini. A vanishing viscosity approach to a rate-independent damage model. *Math. Models Methods Appl. Sci.*, 23(4):565–616, 2013.

[7] D. Knees, R. Rossi, and C. Zanini. A quasilinear differential inclusion for viscous and rate-independent damage systems in non-smooth domains. *Nonlinear Anal. Real World Appl.*, 24:126–162, 2015.

[8] D. Knees and A. Schröder. Computational aspects of quasi-static crack propagation. *Discrete Contin. Dyn. Syst. Ser. S*, 6(1):63–99, 2013.

[9] A. Mielke, R. Rossi, and G. Savaré. Balanced viscosity (BV) solutions to infinite-dimensional rate-independent systems. *J. Eur. Math. Soc. (JEMS)*, 18(9):2107–2165, 2016.

[10] A. Mielke and T. Roubíček. Rate-independent damage processes in nonlinear elasticity. *Math. Models Methods Appl. Sci.*, 16(2):177–209, 2006.

[11] A. Mielke and T. Roubíček. *Rate-independent systems*, volume 193 of *Applied Mathematical Sciences*. Springer, New York, 2015. Theory and application.

[12] A. Mielke, F. Theil, and V. I. Levitas. A variational formulation of rate-independent phase transformations using an extremum principle. *Arch. Ration. Mech. Anal.*, 162(2):137–177, 2002.
[13] M. Thomas and A. Mielke. Damage of nonlinearly elastic materials at small strain – existence and regularity results. *ZAMM, Z. Angew. Math. Mech.*, 90(2):88–112, 2010.

Buckling behind brittle fracture in soft solids

Davide Riccobelli
(joint work with Pasquale Ciarletta, Guido Vitale, Corrado Maurini, Lev Truskinovsky)

In problems involving the propagation of pre-existing cracks, the linearized theory of elasticity is commonly employed. However, we present evidence that crack nucleation in soft materials requires the consideration of both geometrically and physically nonlinear elasticity.

In this respect, we analyze a simple model of the traction of an elastic block $[-L,\, L] \times [0, H]$, as shown in Fig. 1 (left), exhibiting stress softening. The body is assumed to be incompressible and homogeneous. The block is stretched along the $\boldsymbol{e}_1$ direction with a mean stretch λ. The energy of the material can be described by means of a scalar function $W(\mathsf{F}) = w(\lambda_1)$, where F is the deformation gradient and λ_1 is its greatest principal value. The key assumption in the model is that the material exhibits softening at large strains, so that $w''(\lambda_1) < 0$ for $\lambda > \lambda_{\mathrm{lm}}$, where $\lambda_{\mathrm{lm}} > 1$ is a given stretch.

The force balance is given by $\nabla \cdot \mathsf{P} = 0$, where P_{ij} are the components of the first Piola-Kirchhoff stress tensor P. On the side boundaries $x_1 = \pm L$ we impose $y_1 = \pm \lambda L$ together with the free sliding condition $P_{12} = 0$; the upper boundary $x_2 = 0$ is assumed to be free so that $P_{22} = P_{21} = 0$; the lower boundary $x_2 = H$ will be constrained only vertically so that $y_2 = H/\lambda$ and $P_{21} = 0$. It can be easily shown that the homogeneous deformation $\boldsymbol{y}(\boldsymbol{X}) = \lambda X_1 \boldsymbol{e}_1 + \lambda^{-1} X_2 \boldsymbol{e}_2$ is always

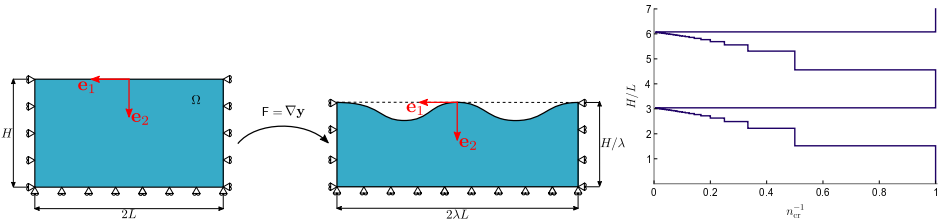

Figure 1. (Left) Schematic representation of the considered surface instability showing the reference and the actual configurations, detailing the nature of the boundary conditions. (Right) Inverse of the critical buckling wavenumber n_{cr} versus the aspect ratio H/L.

a solution of the nonlinear elastic problem quasi-static deformations and $w'(\lambda)$ is the stress along the direction of traction.

We explore both linear and nonlinear stages of the bifurcations of the homogeneous solution [2]. By means of the method of incremental deformations, we show that the block can undergo a sequence of elastic instabilities. For each aspect ratio H/L, an infinite number of bifurcations takes place in the interval $\lambda_{\rm lm} \leq \lambda \leq \lambda_{\rm cc}$. The stretch $\lambda_{\rm lm}$ corresponds to the Considère or the load maximum threshold, i.e. the maximum value of the axial stress $w'(\lambda)$. The other end of the interval, $\lambda_{\rm cc}$, corresponds to the violation of the complementing condition, namely the stretch at which the homogeneous traction of the block becomes unstable in the limit $H, L \to \infty$. The resulting bifurcation diagram is remarkably unconventional, exhibiting an exceptional sensitivity to the aspect ratio H/L, which recalls the transition to turbulence in fluids, see Fig. 1 (right).

The behavior close to the bifurcation point is analyzed close to the bifurcation point through a weakly nonlinear analysis. The system exhibits two types of bifurcations: if the bifurcation point is close to $\lambda_{\rm lm}$, a diffuse necking takes place, conversely if the critical stretch is close to $\lambda_{\rm cc}$ a surface wrinkling is observed. In all the cases analyzed in the study, the bifurcation is subcritical.

Finite element simulations are exploited to explore the fully non-linear regime. The bifurcation diagram is reconstructed by using a pseudo-arclength continuation method. The elastic model is simulated until the limit of its validity, i.e. until the violation of the complementing condition, where strain localization takes place at the free surface, marking the onset of the formation of the cracks. The emerging strain singularities make scale-free continuum elasticity inadequate. In order to go beyond such a point, a regularization inspired by gradient damage models of fracture is introduced [1]. The resulting post-buckling evolution shows the gradual localization of the deformation in sharp regions, which precedes the actual formation of cracks, see Fig. 2.

References

[1] J. J. Marigo, C. Maurini, K. Pham, *An overview of the modelling of fracture by gradient damage models*, Meccanica **51** (2016), 3107-3128.

[2] D. Riccobelli, P. Ciarletta, G. Vitale, C. Maurini, L. Truskinovsky, *Elastic instability behind brittle fracture in soft solids*, arXiv preprint (2023) arXiv:2311.17372.

Crack nucleation in variational gradient damage models endowed with a local minimization principle

Corrado Maurini

Phase-field models of fracture originate variational regularization of the Griffith brittle fracture model [1]. The variational approach to fracture has established a precise link between the toughness of the sharp interphase Griffith model and that of the smeared phase-field model, in terms of the convergence of the global minima of the energy (Gamma-convergence). However, brittle fracture is characterized by two key material parameters: fracture toughness and strength. Fracture

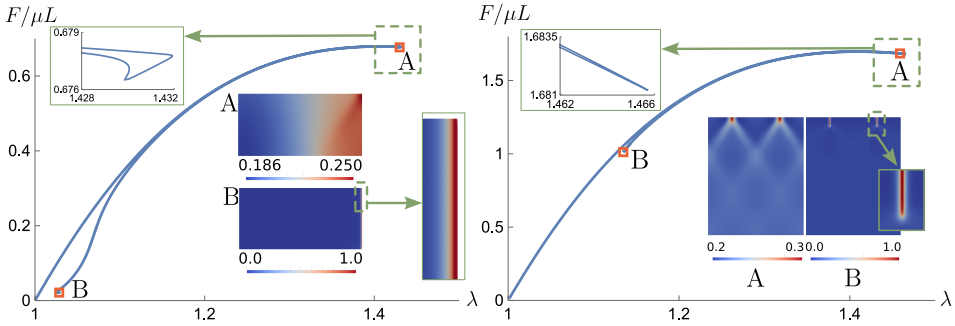

FIGURE 2. Normalized axial force $F/\mu L$ versus the mean stretch λ for the near necking case ($H/L = 1$, left) and the near wrinkling cae ($H/L = 2.5, right$). The insets on the right show the distribution of the phase field variable α in the reference configuration corresponding to the points A and B. The parameter $\ell_0/H = 0.01$.

toughness is the energy dissipated during crack propagation, while strength is the maximum allowable stress that the material can sustain before failure through crack nucleation. From the energetic viewpoint, the strength can be related to the energy barrier between the purely elastic solution and the solution with cracks, an information that Gamma-convergence cannot provide. Currently, whether and how phase-field approaches can correctly account for strength and crack nucleation criteria is a matter of debate.

Differing from the global minimization formulation at the basis of Gamma-convergence results, we consider quasi-static evolution based on the directional local minimization principle. In this framework, we relate the length-scale introduced in phase-field models to the stability margin of local energy minima, and thus to the nucleation thresholds [3, 2, 4]. This viewpoint enables us to understand crack nucleation phenomena and the morphogenesis of complex crack patterns as a structural stability problem [4]. The crack nucleation threshold is identified as the loss of stability of the purely elastic solution or solutions with diffused damage. The first order optimality conditions for the phase-field energy functional give a damage criterion, that can be regarded as the elemental necessary conditions for crack nucleation. We discuss also second-order optimality conditions providing necessary or sufficient criteria for the (in)stability. Hence, we present an algorithm to test these conditions numerically and illustrate it in meaningful examples [4].

Finally, we address the problem of crack nucleation under multi-axial loading. The theoretical stability analysis discloses the subtle influence of softening, energy decompositions, and loading modes on the strength observed in numerical simulations. To address the limitations of existing approaches, we combine variational phase-field models and nonlinear elasticity, with a focus on the case of crack nucleation in almost incompressible materials.

References

[1] B. Bourdin, G.A. Francfort, J.-J. Marigo, *The variational approach to fracture.* J. Elasticity **91** (2008), 5–148.

[2] E.Tanné, T.Li, B.Bourdin, J.-J. Marigo, C. Maurini, *Crack nucleation in variational phase-field models of brittle fracture.* Journal of the Mechanics and Physics of Solids, **110** (2018).

[3] B. Bourdin, J.-J. Marigo, C. Maurini, P.Sicsic, *Morphogenesis and propagation of complex cracks induced by thermal shocks.* Phys. Rev. Lett. **112** (1), 014301 (2014).

[4] A. A. León Baldelli, C. Maurini, *Numerical bifurcation and stability analysis of variational gradient-damage models for phase-field fracture.* Journal of the Mechanics and Physics of Solids, **152** (2021).

[5] L. De Lorenzis, C.Maurini, *Nucleation under multi-axial loading in variational phase-field models of brittle fracture.* International Journal of Fracture (2022).

[6] A.Kumar, B. Bourdin, G.A. Francfort, O. Lopez-Pamies, *Revisiting nucleation in the phase-field approach to brittle fracture*, Journal of the Mechanics and Physics of Solids, **142** (2020).

On the use of image correlation techniques for the analysis of fracture

François Hild

(joint work with the Eikology group of LMPS)

The analysis of fracture involves kinematic fields that have special features, which call for measurement techniques that enable damage to be quantified. Among all optical techniques, digital image correlation (DIC) has become one of the most popular choices [1]. The aim of the presentation is to introduce the general principles of DIC for the registration of 2D images, its extension to that of 3D images (i.e., digital volume correlation [2]), and applications dealing with damage and failure.

Digital image correlation (DIC) was introduced in the early 1980s [3]. Very early on, its use to analyze cracks under quasi-static and dynamic propagation conditions was recognized [4, 5] and further confirmed over the years [6, 7]. The first versions of DIC were based on local registrations with small interrogation windows. In the first decade of the twenty first century, global approaches were proposed, in which large regions of interest were registered when the displacement field was, for instance, parameterized with finite element discretizations [8, 9]. Enriched kinematics was then included [10] to account for displacement discontinuities induced by cracks. To mitigate displacement fluctuations due to measurement uncertainties, elastic regularization was added in the total cost function to be minimized [11]. Another route is to use closed-form solutions (e.g., Williams' series [12]) as the kinematic basis of global DIC to directly extract fracture mechanics parameters from images. Such an approach corresponds to integrated DIC [13] in which the measured displacement fields are mechanically admissible. It has very recently been extended to spacetime formulations to calibrate phase field parameters [14].

With the democratization of X-ray tomography, digital volume correlation (DVC) has been applied to register 3D (reconstructed) volumes. The first implementation was also local in space [2]. It was then generalized to global DVC [15]. One of the very first applications was on the extraction of stress intensity factor

profiles from measured 3D displacement fields [16]. DVC was also enriched (as in DIC) to deal with displacement discontinuities induced by cracks [17]. Regularized DVC was then introduced [18]. Subsequently, heterogeneous regularization was considered to account for the presence of different elastic phases. Damage was included to quantify degradation mechanisms in mortar [19]. The fracture energy of a phase field model could also be calibrated at the microscale and the damaged zones were rather well predicted when the measured boundary conditions were applied to the numerical models [20].

These various examples illustrate how DIC/DVC provided thorough means for validating damage and fracture models.

References

[1] M. Sutton, J. Orteu, H. Schreier, *Image correlation for shape, motion and deformation measurements: Basic Concepts, Theory and Applications* (Springer, New York, NY (USA), 2009)

[2] B. Bay, T. Smith, D. Fyhrie, M. Saad, Digital volume correlation: Three-dimensional strain mapping using X-ray tomography, Experimental Mechanics **39**, 217 (1999)

[3] T. Chu, W. Ranson, M. Sutton, W. Peters, Applications of digital-image-correlation techniques to experimental mechanics, Experimental Mechanics **3**(25), 232 (1985)

[4] W. Peters, W. Ranson, J. Kalthoff, S. Winkler, A study of dynamic near-crack-tip fracture parameters by digital image analysis, Journal de Physique Colloques **46**(C5), 631 (1985)

[5] S. McNeill, W. Peters, M. Sutton, Estimation of stress intensity factor by digital image correlation, Engineering Fracture Mechanics **28**(1), 101 (1987)

[6] S. Roux, J. Réthoré, F. Hild, Digital image correlation and fracture: An advanced technique for estimating stress intensity factors of 2D and 3D cracks, Journal of Physics D: Applied Physics: Appl. Phys. **42**, 214004 (2009)

[7] F. Hild, A. Bouterf, S. Roux, Damage Measurements via DIC, International Journal of Fracture **191**(1-2), 77 (2015)

[8] Y. Sun, J. Pang, C. Wong, F. Su, Finite-element formulation for a digital image correlation method, Applied Optics **44**(34), 7357 (2005)

[9] G. Besnard, F. Hild, S. Roux, "Finite-element" displacement fields analysis from digital images: Application to Portevin-Le Chatelier bands, Experimental Mechanics **46**, 789 (2006)

[10] J. Réthoré, F. Hild, S. Roux, Extended digital image correlation with crack shape optimization, International Journal for Numerical Methods in Engineering **73**(2), 248 (2008)

[11] J. Réthoré, S. Roux, F. Hild, An extended and integrated digital image correlation technique applied to the analysis fractured samples, European Journal of Computational Mechanics **18**, 285 (2009)

[12] M. Williams, On the stress distribution at the base of a stationary crack, ASME Journal of Applied Mechanics **24**, 109 (1957)

[13] S. Roux, F. Hild, Stress intensity factor measurements from digital image correlation: post-processing and integrated approaches, International Journal of Fracture **140**(1-4), 141 (2006)

[14] V. Kosin, A. Fau, C. Jailin, F. Hild, T. Wick, Parameter identification of a phase-field fracture model using integrated digital image correlation, Computer Methods in Applied Mechanics and Engineering **420**, 116689 (2024)

[15] S. Roux, F. Hild, P. Viot, D. Bernard, Three dimensional image correlation from X-Ray computed tomography of solid foam, Composites Part A: Applied Science and Manufacturing **39**(8), 1253 (2008)

[16] N. Limodin, J. Réthoré, J. Buffière, A. Gravouil, F. Hild, S. Roux, Crack closure and stress intensity factor measurements in nodular graphite cast iron using 3D correlation of laboratory X ray microtomography images, Acta Materialia **57**(14), 4090 (2009)

[17] J. Rannou, N. Limodin, J. Réthoré, A. Gravouil, W. Ludwig, M. Baïetto, J. Buffière, A. Combescure, F. Hild, S. Roux, Three dimensional experimental and numerical multiscale analysis of a fatigue crack, Computer Methods in Applied Mechanics and Engineering **199**, 1307 (2010)
[18] T. Taillandier-Thomas, S. Roux, T. Morgeneyer, F. Hild, Localized strain field measurement on laminography data with mechanical regularization, Nuclear Instruments and Methods in Physics Research Section B **324**, 70 (2014)
[19] A. Tsitova, F. Bernachy-Barbe, B. Bary, S. Al Dandachli, C. Bourcier, B. Smaniotto, F. Hild, Damage Quantification via Digital Volume Correlation with Heterogeneous Mechanical Regularization: Application to an In Situ Meso-Flexural Test on Mortar, Experimental Mechanics **62**, 333 (2022)
[20] A. Tsitova, F. Bernachy-Barbe, B. Bary, C. Bourcier, F. Hild, Identification of microscale fracture models for mortar with in-situ tests, International Journal of Mechanical Sciences **242**, 107988 (2023)

Length-scales in peridynamic models of quasi-static and dynamic fracture

Florin Bobaru

I will present some recent results on dynamic fracture at an interface [1]. The location and properties of a material interface in PMMA bonded samples has a strong influence on whether a dynamic crack runs along the interface before punching through the second PMMA layer or not. A peridynamic (PD) model that only approximately represents the actual thickness of the interface can, nevertheless, correctly predict the experimentally observed behavior. The peridynamic horizon size, in this case, does not have to be smaller than the interface thickness to allow us to obtain accurate results. Once the PD horizon is sufficiently close (one order of magnitude) to the actual thickness of the interface, the results are relatively insensitive to its size. The situation is quite different for the case of a thin, hot glass plate with a notch, slowly immersed in cold water. In this case, a quasi-static crack may grow from the notch and propagate straight, or oscillate in its path, or even branch (but not from its tip!), depending on the immersion speed (micrometers to tens of micrometers per second) and the plate width, for example. We show that for this quasi-static crack growth induced by thermal stresses, the PD horizon size must be carefully determined from one experimental data point, to fully predict an entire phase diagram of experiments for various plate widths and immersion speeds [2]. In this case, finding the proper PD horizon size to match material length-scales induced by the sample geometry and thermal loading conditions is essential to predicting the correct failure behavior. If time permits, I will also discuss fast solvers for PD models in dynamic and quasi-static brittle and ductile fracture [3].

References

[1] L. Wang, J. Mehrmashhadi, and F. Bobaru, *Interfaces in dynamic brittle fracture of PMMA: a peridynamic analysis.* (International Journal of Fracture, 2023)
[2] Z. Xu., G. Zhang, Z. Chen, and F. Bobaru, *Elastic vortices and thermally-driven cracks in brittle materials with peridynamics.* (International Journal of Fracture 209, 203–222, 2018)

[3] S. Jafarzadeh, F. Mousavi, L. Wang, and F. Bobaru, *A MATLAB Code for Explicit Fast Convolution-based Peridynamic Analysis of Deformation and Fracture.* (Journal of Peridynamics and Nonlocal Modeling, 2023)

Variational fracture and loads: a local variational principle for fracture

Christopher J. Larsen

We consider for simplicity scalar displacements u on $\Omega \subset \mathbb{R}^N$ with the simplest elastic energy density $\frac{1}{2}|\nabla u|^2$, Griffith constant G_c, and crack sets K. The total energy of a displacement-crack pair (u, K), with u allowed to be discontinuous across K, is given by [2]

$$E^G(u, K) := \frac{1}{2}\int_\Omega |\nabla u|^2 dx + G_c \mathcal{H}^{N-1}(K),$$

where $\mathcal{H}^{N-1}(K)$ is the $N-1$ dimensional Haudorff measure (surface area) of the crack K. Minimizing this energy (globally or locally) subject to a given displacement boundary condition produces a displacement u and crack set K satisfying a form of Griffith stability:

$$E^G(u, K) \leq E^G(v, \kappa)$$

for pairs (v, κ) satisfying $v = u$ on $\partial\Omega$ and $\kappa \supset K$. If (u, K) are obtained by global minimization, then this inequality holds for all such (v, κ), and if they are obtained by local minimization, then the inequality will hold if v is sufficiently close to u.

We now turn to the problem of including boundary and body loads in variational fracture. With boundary load f on part of $\partial\Omega$ denoted $\partial_N\Omega$, and displacement boundary condition zero, for example, on the remainder of the boundary $\partial_D\Omega$, it would seem that we should minimize

$$E_{Load}(u, K) := \frac{1}{2}\int_\Omega |\nabla u|^2 dx - \int_{\partial_N\Omega} fu\, ds + G_c \mathcal{H}^{N-1}(K)$$

over $u \in H^1(\Omega \setminus K)$ (a slight abuse of notation) with $u = 0$ on $\partial_D\Omega$. Minimizing this energy is easily seen to be impossible (except in the trivial case $f \equiv 0$). The idea is, we can choose a part of $\partial_N\Omega$ in which the average of f is not zero, and if we create a crack disconnecting that part of the boundary from $\partial_D\Omega$, the second term in the energy can be sent $-\infty$ with a controlled cost in the rest of the energy, so the total energy goes to $-\infty$. Essentially the same issue occurs with body loads.

But this problem is not present if we want the crack surface energy to compete with elastic energy the same way it does with displacement boundary conditions, as we advocated in [4]. There, we showed that this principle can be implemented with boundary loads – instead of trying to minimize a single energy, we can simultaneously minimize two different energies:

$$\frac{1}{2}\int_\Omega |\nabla u|^2 dx - \int_{\partial_N\Omega} fu\, ds$$

over displacements with the same crack, and

$$\frac{1}{2}\int_\Omega |\nabla u|^2 dx + G_c \mathcal{H}^{N-1}(K)$$

over displacements with the same displacement boundary condition even on $\partial_N \Omega$. We then get the elastic plus load equilibrium u we want, but the crack results only from competition between elastic and surface energy (of course, the crack indirectly depends on the load, but only by the dependence of u on the load, and not direct energy competition between the load and surface area). This formulation, and a method for showing existence, are developed in [4].

This kind of dual minimality will not work for body loads, however. We still want a dual variational principle – one for determining the equilibrium displacement, and one with competition between elastic and surface energy, but the latter variational principle must be local.

In addition to treating body loads, a local variational principle is necessary in order to combine Griffith (sharp) fracture with strength [3], treat viscoelastic materials [6], as well as study implementations of phase-field fracture [1].

Our local variational principle [5] is based on the idea that under a certain rescaling, blow-up limits of stable states must have a global minimality property, which we state for $\Omega \subset \mathbb{R}^2$ for simplicity. Given a displacement-crack pair (u, K), for $x_0 \in \Omega$ fixed, we set

$$u_\varepsilon(x) := \varepsilon^{-\frac{1}{2}}[u(x_0 + \varepsilon x) - u(x_0)] \text{ and } K_\varepsilon := \varepsilon^{-1}(K - x_0). \tag{1}$$

If a pair $(\hat{u}, \hat{K})$ is the limit as $\varepsilon \to 0$ of the above, then we consider the following minimality for this pair:

Definition 1 (Global Griffith stability)**.** $(\hat{u}, \hat{K})$ with $\hat{u} \in H^1_{loc}(\mathbb{R}^2 \setminus \hat{K})$ is *globally Griffith-stable* if for every $r > 0$, it minimizes

$$E^G_r(w, \kappa) := \frac{1}{2}\int_{B(0,r)} |\nabla w|^2 dx + G_c \mathcal{H}^1(\kappa \cap B(0, r))$$

over pairs (w, κ) satisfying $w \in H^1_{\hat{u}}(B(0, r) \setminus \kappa)$ and $\kappa \supset \hat{K} \cap B(0, r)$. Here, $\mathcal{H}^1$ is the one-dimensional Hausdorff measure.

Our main definition then just requires all such blow-up limits to have this minimality:

Definition 2 (Local Griffith stability)**.** (u, K) is *locally Griffith stable* if for every $x_0 \in \Omega$, every blow-up limit $(\hat{u}, \hat{K})$ of $(u_\varepsilon, K_\varepsilon)$ is globally Griffith stable.

This is then combined with the elastic equilibrium variational principle:

Definition 3 (elastic-Griffith stability)**.** (u, K) with $u \in H^1(\Omega \setminus K)$ is elastic-Griffith stable if:

(1) u minimizes

$$w \mapsto \frac{1}{2}\int_\Omega |\nabla w|^2 dx$$

over $w \in H^1(\Omega \setminus K)$ with $w = u$ on $\partial\Omega$, i.e.,

$$\Delta u = 0 \text{ in } \Omega \setminus K,\ \partial_\nu u = 0 \text{ on } K,$$

and

(2) (u, K) is locally Griffith stable (Definition 2).

Body and boundary loads are easily added:

Definition 4 (elastic-Griffith stability with loads)**.**
We say (u, K) with $u \in H^1(\Omega \setminus K)$ is elastic-Griffith stable with body load f and boundary load g (applied to part of the boundary $\partial_N\Omega$) if:

(1) u minimizes

$$w \mapsto \frac{1}{2}\int_\Omega |\nabla w|^2 dx - \int_\Omega fw\, dx - \int_{\partial_N\Omega} gw\, ds$$

over $w \in H^1(\Omega \setminus K)$ with $w = u$ on $\partial_D\Omega := \partial\Omega \setminus \partial_N\Omega$, i.e.,

$$\Delta u = f \text{ in } \Omega \setminus K,\ \partial_\nu u = 0 \text{ on } K, \text{ and } \partial_\nu u = g \text{ on } \partial_N\Omega,$$

and

(2) (u, K) is locally Griffith stable.

Incorporating viscoelasticity, and the connection to phase-field fracture, are also discussed.

Acknowledgments. This material is based on work supported by the National Science Foundation under Grant No. DMS-2206114.

References

[1] Bourdin, B.; Francfort, G. A.; Marigo, J.J.: Numerical experiments in revisited brittle fracture. *J. Mech. Phys. Solids*, **48-4**, 797-826, 200.
[2] Francfort, G. A., Marigo, J.J. Revisiting brittle fracture as an energy minimization problem. *J. Mech. Phys. Solids*, **46-8**, 1319-1342, 1998.
[3] Kumar A, Francfort GA, Lopez-Pamies O (2018). Fracture and healing of elastomers: A phase-transition theory and numerical implementation. *J. Mech. Phys. Solids* 112:523–551.
[4] Larsen, C. J. Variational fracture with boundary loads. *Appl. Math. Lett.* **121** (2021), 107437.
[5] Larsen, C. J. A local variational principle for fracture. arXiv: 2402.08633 (2024).
[6] Shrimali, B., Lopez-Pamies, O. The "pure-shear" fracture test for viscoelastic elastomers and its revelation on Griffith fracture, *Extreme Mechanics Letters*, **58**, (2023) 101944.

Peridynamic modeling of the interplay of wave propagation and dynamic fracture

Kai Partmann (PhD student talk)

Peridynamics is particularly well-suited for modeling discontinuities such as cracks due to its integro-differential equation. In this study, we investigate the interplay between wave propagation and dynamic fracture, focusing on a comparative analysis of different material formulations within the peridynamics framework. Our research focuses on three material formulations: continuum-kinematics-based peridynamics, non-ordinary state-based peridynamics, and bond-associated non-ordinary state-based peridynamics. Each formulation has unique advantages and challenges. Continuum-kinematics-based peridynamics, while conceptually sound, suffers from the surface effect and is computationally very expensive. Non-ordinary state-based peridynamics, although promising, exhibit instabilities, especially when dealing with cracks. In contrast, bond-associated non-ordinary state-based peridynamics emerges as a promising candidate, demonstrating stability and good results. Using examples from wave propagation and dynamic fracture, we demonstrate the differences between these formulations with different numerical results and compare them to analytical solutions.

Phase-field modeling of fracture: nucleation, dissipation, large deformation, and complex stress states

Kaushik Dayal
(joint work with Janel Chua, George Gazonas, Maryam Hakimzadeh, Carlos Mora-Corral, Noel Walkington)

The growth of cracks is challenging for numerical methods due to the numerous singular surfaces that must be tracked. Phase-field modeling provides an attractive alternative: by smearing out the singularities appropriately, it is possible to use standard numerical techniques, such as the finite element method, to model cracks that grow in complex ways. While current phase-field models of fracture are widely applied to various types of engineering problems, they have some critical shortcomings. Specifically, the model parameters that govern the nucleation of cracks is unclear; the behavior of fast moving cracks is unphysical near the sonic velocity; and the material response is unphysical in the large-deformation setting when the crack closes under compressive loading. To address these issues, we present results on a conservation law structure for the phase-field that enables us to transparently incorporate nucleation and stick-slip kinetics; the role of viscous stresses that, while small, are essential to provide regularity near the sonic velocity; and the formulation of a crack strain energy density that appropriately mimics the behavior of a crack under compression and other complex stress states.

References

[1] Hakimzadeh, M., Agrawal, V., Dayal, K. & Mora-Corral, C. Phase-field finite deformation fracture with an effective energy for regularized crack face contact. *Journal Of The Mechanics And Physics Of Solids.* **167** pp. 104994 (2022)

[2] Chua, J., Agrawal, V., Breitzman, T., Gazonas, G. & Dayal, K. Phase-field modeling and peridynamics for defect dynamics, and an augmented phase-field model with viscous stresses. *Journal Of The Mechanics And Physics Of Solids.* **159** pp. 104716 (2022)

[3] Agrawal, V. & Dayal, K. Dependence of equilibrium Griffith surface energy on crack speed in phase-field models for fracture coupled to elastodynamics. *International Journal Of Fracture.* **207** pp. 243-249 (2017)

[4] Chua, J., Karimi, M., Kozlowski, P., Massoudi, M., Narasimhachary, S., Kadau, K., Gazonas, G. & Dayal, K. Deformation Decomposition versus Energy Decomposition for Chemo-and Poro-Mechanics. *Journal Of Applied Mechanics.* **91**, 014501 (2024)

The Brazilian Test: Understanding the Interplay Between Strength and Fracture

John E. Dolbow

(joint work with Oscar Lopez-Pamies)

The Brazilian test has become a standard approach to indirectly measure the tensile strength of brittle materials with relatively large compressive strengths. The test is simple to set up and execute, and it readily lends itself to theoretical analysis. It consists of a circular disk of the material loaded in compression (Figure 1) until it fails, typically via a sudden fracture that splits the specimen in two.

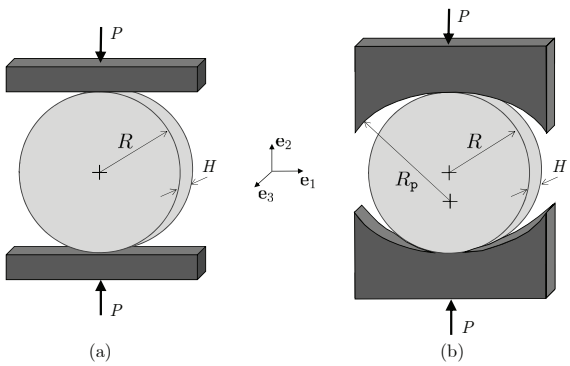

Figure 1. Schematics of the Brazilian test for a specimen of radius R and thickness H under two standard types of loading configurations: (a) flat loading platens and (b) curved loading platens with radius of curvature $R_{\mathfrak{p}}$.

Although mostly used in quasi-static loading, versions of the test where the specimen is impulsively loaded are also employed. While relatively simple to understand, the test has proven elusive to various models for fracture. This is no

doubt due to the fact that the test represents a problem of crack nucleation, particularly under a significant degree of compression. As such it explores a region of parameter space that is rarely the focus of model development for fracture mechanics. What is perhaps under-appreciated is the extent to which this oversight has permitted for the development and acceptance of standardized expressions for strength that can be widely inaccurate. For example, the International Society for Rock Mechanics [2] proposes the use of the formula

$$\sigma_{\mathtt{ts}} = \frac{P_{max}}{\pi RH} \tag{1}$$

to deduce the tensile strength $\sigma_{\mathtt{ts}}$ from the test. In this expression, P_{max} stands for the maximum applied load indicated by the testing machine, while R is the radius of the disk and H is its thickness; see Figure 1.

In this talk, I will highlight our recent work [1] that includes a complete quantitative analysis of where and when fractures nucleate and propagate in Brazilian tests and how to appropriately interpret their results. This is accomplished by deploying the revisited phase-field fracture theory [3] and its recent specialization to compressive loads [4]. This theory is particularly well-suited to analyze the Brazilian test as it allows for the accounting of arbitrary material strength surfaces as well as the transition from crack nucleation to Griffith-like fracture.

The analysis indicates that the point of fracture in a standard Brazilian test coincides with a region of the strength surface that is far from uniaxial tension. By accounting for this basic observation, a modification to the standard formula 1 for material strength arises. The extrapolated result for $\sigma_{\mathtt{ts}}$ is given by the formula

$$\sigma_{\mathtt{ts}} = f\left(P_{max}, \sigma_{\mathtt{cs}}\right) \frac{P_{max}}{\pi RH}, \tag{2}$$

where $f\left(P_{max}, \sigma_{\mathtt{cs}}\right)$ is a factor that, as indicated by its arguments, depends on the maximum force P_{max} measured in the test and the uniaxial compressive strength $\sigma_{\mathtt{cs}}$ of the material. It is given by the fully explicit expression

$$f\left(P_{max}, \sigma_{\mathtt{cs}}\right) = \frac{\left(\sqrt{13} - 2\right) \dfrac{\pi RH}{P_{max}} \sigma_{\mathtt{cs}}}{\dfrac{2\pi RH}{P_{max}} \sigma_{\mathtt{cs}} - \sqrt{13} - 2}. \tag{3}$$

The corrected expression was tested against simulations of Brazilian tests for three materials with compressive-to-tensile strength ratios $\sigma_{\mathtt{cs}}/\sigma_{\mathtt{ts}} = 5, 8$, and 20. For all three materials, the formula (2) yields results for the uniaxial tensile strength $\sigma_{\mathtt{ts}}$ that are within 5% of the exact values.

References

[1] A. Kumar, Y. Liu, J.E. Dolbow, and O. Lopez-Pamies, *The strength of the Brazilian fracture test*, Journal of the Mechanics and Physics of Solids **182** (2024), 105473.

[2] International Society for Rock Mechanics. *Suggested methods for determining tensile strength of rock materials*, Int. J. Rock Mech. Min. Sci. Geomech. **15** (1978), 99–103.

[3] A. Kumar, B. Bourdin, G.A. Francfort, and O. Lopez-Pamies, *Revisiting nucleation in the phase-field approach to brittle fracture*, J. Mech. Phys. Solids **142** (2020), 104027.

[4] A. Kumar, K. Ravi-Chandar, and O. Lopez-Pamies., *The revisited phase-field approach to brittle fracture: Application to indentation and notch problems*, Int. J. Fracture **237** (2022), 83–100.

Different peridynamic approaches to wave propagation and dynamic fracture

Kerstin Weinberg

(joint work with Kai Partmann and Christian Wieners)

Peridynamics is a non-local continuum mechanics formulation that originally describes the interactions between material points with only one spring-like stiffness parameter. Thus, this standard bond-based model is not consistent with classical linear elasticity, and several extensions have been introduced since. In this contribution, we compare different current peridynamic material formulations and their ability to model wave propagation.

In general, the position of a material point inside a body $\mathcal{B}_0$ is described in a reference placement as $\boldsymbol{X}$ and in its current position as

$$\boldsymbol{x} = \boldsymbol{X} + \boldsymbol{u} \tag{1}$$

with the displacement $\boldsymbol{u}(\boldsymbol{X})$. In peridynamics, material points interact with other points inside of their a *neighborhood* $\mathcal{H}$, which is defined as the set of points inside a sphere with the radius $\delta \in \mathbb{R}^+$, also named the *horizon*. The interaction of the point $\boldsymbol{X}$ with its neighbor $\boldsymbol{X}'$ is called *bond* and in reference and current placement it is defined as

$$\boldsymbol{\Delta X} = \boldsymbol{X}' - \boldsymbol{X} \ , \qquad \boldsymbol{\Delta x} = \boldsymbol{x}' - \boldsymbol{x} \ . \tag{2}$$

The evaluation of the bond interactions for all $\boldsymbol{X} \in \mathcal{B}_0$ results in the peridynamic integro-differential equation of motion.

In peridynamics, the continuum is typically point-wise discretized, which, together with the underlying non-local continuum mechanics formulation, makes it ideally suited for dynamic fracture simulation. An important implication in terms of spallation is the correct treatment of elastic waves, such as pressure and stress waves inside a body, which result from an impact or impulse. This motivated us to investigate and compare the elastic wave propagation behavior of a bond-based peridynamic, a continuum-kinematics-based peridynamic, and a non-ordinary state-based peridynamic formulation. We found significant differences in the ability of the different formulations to map the material under dynamic loading, cf. [1, 2].

Using the example of a longitudinal pressure wave inside an elastic bar, we show that the peridynamic formulations are able to reproduce the classical solutions to a different extent. Figure 1 illustrates the wave propagating in a long bar discretized with $10 \times 10 \times 1000$ material points. The wave travels from the left to the right through the bar and has crossed the bar after approximately $t = 0.05$ ms for the first time. The right end of the bar is free, so the displacement amplitude $\hat{u}_x$ increases when the wave front reflects at the boundary. The displacement

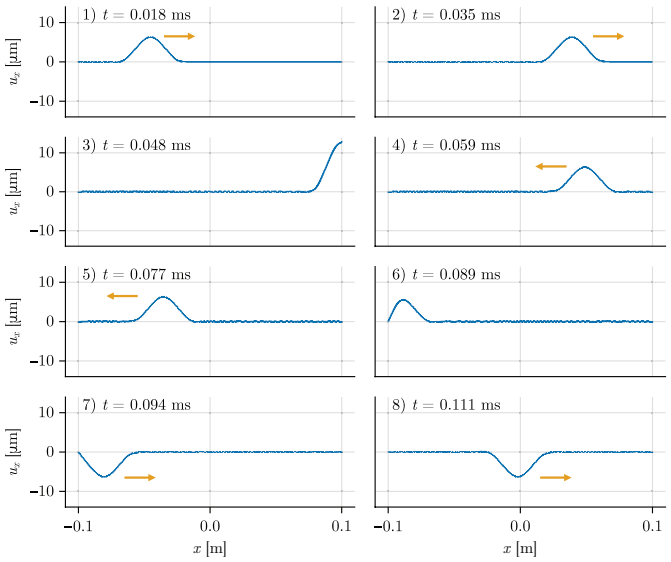

FIGURE 1. Wave traveling through a bar at different instances of time

amplitude $\hat{u}_x$ has the same value after the reflection at the free end, and changes to $-\hat{u}_x$ after the reflection at the fixed end, i.e. the left boundary of the bar.

Further studies show that the bond-based and continuum-kinematics-based formulations can handle wave propagation correctly but suffer largely from the surface effect, i.e. an incomplete horizon. The non-ordinary state-based correspondence formulation does not suffer from the surface effect and models the wave propagation with very high accuracy regarding the wave speed, cf. [3]. However, this formulation does not allow cracks in a straightforward manner.

All simulations are performed with our Julia package `Peridynamics.jl` [4].

REFERENCES

[1] Kai Partmann, Christian Wieners, Kerstin Weinberg. Dynamic fracture with a continuum-kinematics-based peridynamic and a phase-field approach. *Int J Fract*, doi.org/10.1007/s10704-023-00726-7, 2023.

[2] Kai Friebertshäuser, Christian Wieners, Kerstin Weinberg. Dynamic fracture with continuum-kinematics-based peridynamics. *Peridynamics and Its Applications, AIMS Materials Science*, 9(6):791–807, 2022.

[3] Kai Partmann, Manuel Dienst, Kerstin Weinberg. Peridynamic computations of wave propagation and reflection with material interfaces. subm. to *Archive of Applied Mechanics*, 2023.

[4] Kai Partmann, Kerstin Weinberg. Peridynamics.jl. https://doi.org/10.5281/zenodo.8187477, https://github.com/kaipartmann/Peridynamics.jl

Nonlocal gradients in bounded domains motivated by Continuum Mechanics: functional analysis framework and applications in finite and linear elasticity

José Carlos Bellido
(joint work with J. Cueto, C. Mora-Corral)

This is a joint work with J. Cueto and C. Mora Corral. Other collaborators in recent or on-going work are H. Schönberger and P. Radu and M. Foss.

In nonlinear elastostatics, a fundamental question is the existence of equilibrium solutions of the equations of nonlinear elasticity, which often arise as minimizers of the elastic energy

$$\int_\Omega W(x, Du(x))\,dx$$

of a deformation $u : \Omega \to \mathbb{R}^n$. Here Ω is an open bounded subset of $\mathbb{R}^n$ representing the reference configuration of the body (where $n = 3$ is the physically relevant case), and $W : \Omega \times \mathbb{R}^{n\times n} \to \mathbb{R} \cup \{\infty\}$ is the elastic stored-energy function of the material. The usual approach for finding such minimizers is the direct method of the calculus of variations. This theory is well established since the pioneering paper of Ball [1] and its many subsequent refinements.

On the other hand, nonlocal models in solid mechanics have experienced a huge development in the last two decades, especially from the introduction of the peridynamics model by Silling [12]. Many refinements have been introduced since then and, particularly, nonlocal models based on a nonlocal gradient have received a great attention as an adequate substitute of local models.

In general, a nonlocal gradient of a function $u : \Omega \to \mathbb{R}$ takes the form

$$\mathcal{G}_\rho u(x) = \int_\Omega \frac{u(x) - u(y)}{|x - y|} \frac{x - y}{|x - y|} \rho(x - y)\,dy,$$

for a suitable kernel ρ, usually with a singularity at the origin. The choice of ρ determines the nonlocal gradient, which, in turn, specifies the functional space.

The most popular nonlocal gradient is possibly Riesz' s-fractional gradient, which is denoted by $D^s u$ and corresponds to the choices $\Omega = \mathbb{R}^n$ and $\rho(x) = \frac{c_{n,s}}{|x|^{n-1+s}}$ for some constant $c_{n,s}$; see [10, 11]. Here $0 < s < 1$ is the degree of differentiability. While Riesz' fractional gradient enjoys many desirable properties, it has the drawback that the integral defining it is over the whole space, which makes it unsuitable for solid mechanics where the body is represented by a bounded domain $\Omega \subset \mathbb{R}^n$. An adaptation of Riesz' s-fractional gradient for bounded domains was done in [3]. Precisely, for a C_c^∞ function u, its nonlocal gradient is defined as

$$D_\delta^s u(x) = c_{n,s} \int_{B(x,\delta)} \frac{u(x) - u(y)}{|x - y|} \frac{x - y}{|x - y|} \frac{w_\delta(x - y)}{|x - y|^{n-1+s}}\,dy,$$

where w_δ is a fixed function in $C_c^\infty(B(0, \delta))$ satisfying some natural properties to be a truly cut-off function. Here $\delta > 0$ plays the role of the horizon (in the terminology of peridynamics), i.e., the maximum interaction distance.

The existence of minimizers of functionals

$$\int_\Omega W(x, D^s_\delta u(x))\, dx \tag{1}$$

was done in [4] under the assumption of polyconvexity of W (where we also wrote down the corresponding Euler–Lagrange equations), and in [6] under the assumption of quasiconvexity.

Starting with the Euler–Lagrange equations associated to the functional (1). They can be interpreted as the equilibrium equations in nonlocal elasticity. Then we perform a linearization of those equations, which is merely formal, as done classically in texts of elasticity. As expected, the linear equations are remarkably similar to the linear ones, just by replacing the local differential operators (notably, gradient, divergence and Laplacian) by their nonlocal counterparts. In a further stage, existence and uniqueness of those linear equations under the same assumptions as in the classical case, namely, the positive definiteness of the elasticity tensor may be proved. This tensor is a local quantity acting on nonlocal gradients. The key ingredient for the well-posedness of the linear equations is a suitable version of Korn's inequality for nonlocal gradients. Our proof of that inequality is based on the classical Korn inequality together with a procedure described in [4] and [6] (and, earlier, in [9] for the case of the Riesz potential) to translate results from the local case to the nonlocal context. Later, in [5] this model is proved to be equivalent to the well-known Eringen's nonlocal model for linear elasticity [7, 8]

In the talk, we review all the theory, starting from Riesz's fractional gradients and Bessel spaces, and existence for polyconvex functionals based on Riesz' fractional gradients and Γ-convergence to their local counterpart. Next, we describe the functional spaces linked to nonlocal gradients $D^s_\delta u$ and the main result in this sense, and again, existence for polyconvex functionals based on those nonlocal gradients. Finally, we obtain by linearization the nonlocal linearly elastic model. We also report on recent work with J. Cueto, M. Foss and P. Radu on some interesting vector analysis results for nonlocal operators in bounded domains, and on-going work on the generalization of nonlocal gradients for general kernels.

References

[1] J. M. Ball, *Convexity conditions and existence theorems in nonlinear elasticity*, Arch. Rational Mech. Anal., 63 (1977), pp. 337–403.

[2] J. C. Bellido, J. Cueto, and C. Mora-Corral, *Fractional Piola identity and polyconvexity in fractional spaces*, Ann. Inst. H. Poincaré C Anal. Non Linéaire, 37 (2020), pp. 955–981.

[3] ———, *Nonlocal gradients in bounded domains motivated by continuum mechanics: Fundamental theorem of calculus and embeddings*. Advances in Nonlinear Analysis, 12(1), 2023.

[4] ———, *Minimizers of nonlocal polyconvex energies in nonlocal hyperelasticity*. Advances in Calculus of Variations, 2023.

[5] ———, *Eringen's model via linearization of nonlocal hyperelasticity*. Mathematics and Mechanics of Solids, 2023.

[6] J. Cueto, C. Kreisbeck, and H. Schönberger, *Variational analysis of integral functionals involving nonlocal gradients on bounded domains*. ArXiv preprint 2302.05569, 2023.

[7] A. C. Eringen, *Nonlocal continuum field theories*, Springer-Verlag, New York, 2002.

[8] A. Evgrafov and J. C. Bellido, *From non-local Eringen's model to fractional elasticity*, Math. Mech. Solids, 24 (2019), pp. 1935–1953.
[9] C. Kreisbeck and H. Schönberger, *Quasiconvexity in the fractional calculus of variations: characterization of lower semicontinuity and relaxation*, Nonlinear Anal., 215 (2022), pp. 112625, 26.
[10] T.-T. Shieh and D. E. Spector, *On a new class of fractional partial differential equations*, Adv. Calc. Var., 8 (2015), pp. 321–336.
[11] ———, *On a new class of fractional partial differential equations II*, Adv. Calc. Var., (2017).
[12] S. A. Silling, *Reformulation of elasticity theory for discontinuities and long-range forces*, J. Mech. Phys. Solids, 48 (2000), pp. 175–209.

On some aspects of optimal control of phase field fracture propagation

Ira Neitzel
(joint work with Andreas Hehl)

In this talk we mainly discuss second order sufficient optimality conditions for a time-discrete but spatially continuous optimal control problem governed by a regularized phase field fracture propagation model problem, cf. [5], with displacement u and phase-field ϕ, controlled by a Neumann-boundary force q. We start by introducing the uncontrolled fracture propagation model problem similar to [7, 8] based on an energy minimization functional with Ambrosio-Tortorelli-regularization, cf. [1].

Since fracture propagation itself is a minimization problem, adding an outer optimal control problem would lead to a bilevel optimization problem, where the fracture irreversibility condition in the lower level problem would introduce specific difficulties when discussing optimality conditions. We therefore regularize the problem to eventually obtain a formulation fitting into the framework of PDE-constrained optimization.

The fracture irreversibility condition is replaced by a penalization term as in [9] in the energy functional, and a viscous regularization, cf. [6], guarantees strict convexity and thus unique solvability of this minimization problem under a size condition of the corresponding regularization parameter that can be interpreted as a smallness-condition on the time-steps in the time-discrete model. Strict convexity of the energy functional then allows to replace this minimization problem by its first order necessary conditions in form of Euler-Lagrange equations. The first time step of these reads as follows:

For a given boundary force q and initial pair of displacement and phase field (u^0, ϕ^0) with $0 \leq \phi^0 \leq 1$, find displacement and phase field $\mathbf{u} = (u, \phi)$, solving

$$
(\mathrm{EL}^{\gamma,\eta}) \qquad \begin{aligned} \Big(g(\phi)\mathbb{C}e(u), e(v)\Big) - (q, v)_{\Gamma_N} &= 0, \\ \epsilon(\nabla\phi, \nabla\psi) - \frac{1}{\epsilon}(1-\phi, \psi) + \eta(\phi - \phi^0, \psi) & \\ +(1-\kappa)(\phi\mathbb{C}e(u) : e(u), \psi) & \\ +\gamma([(\phi - \phi^0)^+]^3, \psi) &= 0. \end{aligned}
$$

Here, ϵ is the phase-field parameter due to the Ambrosio-Tortorelli regularization, η is the viscous regularization parameter, and γ the penalization parameter for the irreversibility conditions. We point out that all parameters remain fixed in this talk. For a convergence analysis with respect to γ, we refer to [8] and [3].

With the forward model at hand, the tracking type optimal control problem

$$(\mathrm{NLP}^{\gamma,\eta}) \qquad \begin{aligned} &\min_{q,\mathbf{u}} J(q,\mathbf{u}) := \frac{1}{2}\|u-u_d\|^2 + \frac{\alpha}{2}\|q\|^2_{\Gamma_N} \\ &\text{s.t. } \mathbf{u} = (u,\phi) \text{ given the data } q, \text{ solves } (\mathrm{EL}^{\gamma,\eta}). \end{aligned}$$

is introduced, where u_d is a given desired displacement and $\alpha > 0$ is the Tikhonov-parameter. Further, control bounds of the form

$$q_a \leq q \leq q_b$$

can be considered. Note that the Euler Lagrange equations are quasilinear, so the overall optimal control problem is nonconvex. For the precise functional analytic setting we refer to [5].

We first give an overview about the challenges of second order sufficient optimality conditions in function spaces and PDE-constrained optimization and some regularity results that are needed, before we show a result on second order sufficient conditions that follows from the abstract theory in [2], once all prerequisites are established. We finish the talk with a short overview on how local convergence of the sequential quadratic programming method can be obtained, cf. [4] for details. This follows from a discussion of Newtons-method for the first order optimality conditions in form of generalized equations, cf. e.q. also the meanwhile classical result in [10]. We indicate in particular the role of second order sufficient optimality conditions.

References

[1] L. Ambrosio and V.M. Tortorelli, *On the approximation of free discontinuity problems*, Boll. Un. Mat. Ital. B (7), **6**(1) (1992), 105–123.

[2] E. Casas, F. Tröltzsch, *Second order analysis for optimal control problems: improving results expected from abstract theory*, SIAM Journal on Optimization, **22** (2012), 261–279.

[3] A. Hehl , M. Mohammadi, I. Neitzel and W. Wollner. *Optimizing fracture propagation using a phase-field approach*, Non-smooth and complementarity-based distributed parameter systems - simulation and hierarchical optimization. In: Internat. Ser. Numer. Math, 172, 329–351, Birkhäuser/Springer (2022).

[4] A. Hehl , I. Neitzel, *Local quadratic convergence of the SQP method for an optimal control problem governed by a regularized fracture propagation model*, SPP1962 preprint, SPP1962–203, (2023).

[5] A. Hehl , I. Neitzel, *Second-order optimality conditions for an optimal control problem governed by a regularized phase-field fracture propagation model*, Opimization, 72(6), 1665–1689, (2023).

[6] D. Knees , R. Rossi and C. Zanini *A vanishing viscosity approach to a rate-independent damage model*, Math. Models Methods Appl. Sci., 23(4), 565–616, (2013).

[7] I. Neitzel, T. Wick and W. Wollner. *An optimal control problem governed by a regularized phase-field fracture propagation model*, SIAM J. Control Optim., 55(4):2271–2288, 2017.

[8] I. Neitzel, T. Wick and W. Wollner. *An optimal control problem governed by a regularized phase-field fracture propagation model. Part II: The regularization limit*, SIAM J. Control Optim., 57(3):1672–1690, 2019.
[9] C. Meyer, A. Rademacher and W. Wollner, *Adaptive optimal control of the obstacle problem*, SIAM J. Sci. Comput., **37**(2) (2015), A918–A945.
[10] F. Tröltzsch. *On the Lagrange-Newton-SQP method for the optimal control of semilinear parabolic equations*, SIAM J. Control. Optim., **38**(1) (1999), 267–288.

Goal oriented error estimation for space-time adaptivity in phase-field fracture

Viktor Kosin (PhD student talk)

In this talk, we introduce a phase-field fracture model in a space-time formulation and use the dual-weighted residual (DWR) method to formulate a goal oriented error estimator for adaptive refinement in space and time. Tensor-product space-time finite elements are being used with continuous elements in space and discontinuous elements in time, such that the primal problem can be solved with a time-stepping scheme. Because the irreversibility condition is solved using an active set method, the time dependency vanishes for the adjoint problem and no backwards time-stepping is needed. The error is localized using partition of unity (PU). The convergence order of the space-time adaptivity is analyzed on numerical tests with different goal functionals.

On the energy decomposition in variational phase-field models for brittle fracture under multi-axial stress states

Laura De Lorenzis
(joint work with Francesco Vicentini, Camilla Zolesi, Pietro Carrara, Corrado Maurini)

Phase-field models of brittle fracture are typically endowed with a decomposition of the elastic strain energy density in order to realistically describe fracture under multi-axial stress states. The major contents and findings of this work can be summarized as follows:

- We define essential requirements for a phase-field model of brittle fracture dealing with multi-axial stress states to correctly describe both nucleation and propagation of cracks. These requirement turn out to be the followng: strain-hardening, stress-softening, tension/compression asymmetry, flexibility (i.e. the ability to independently calibrate not only the uniaxial tensile strength but also the uniaxial compressive strength and the shear strength), and crack-like residual stress.
- In light of these requirements we review some available variational phase-field models of brittle fracture based on energy decomposition, namely the volumetric-deviatoric [1], the spectral [2], the no-tension [3] and the DP-like models [4]. We discuss their advantages and limitations in light of the

identified requirements. None of the analyzed existing decompositions is found to meet all the requirements.

- We propose a new model that we denote as star-convex model. This model, based on a minimal modification of the volumetric-deviatoric decomposition, is equipped with a $\gamma^\star$ parameter that allows independent calibration of compressive and tensile strengths. Such partial flexibility can be extended to the shear strength by modifying the softening laws. Additionally, the model satisfies all other requirements. Thus, it represents a very simple but effective step forward towards the realistic prediction of brittle fracture mechanisms under multiaxial stress states.

References

[1] H. Amor, and J.J. Marigo and C. Maurini, *Regularized formulation of the variational brittle fracture with unilateral contact: Numerical experiments*, Journal of the Mechanics and Physics of Solids **57** (2009), 1209–1229.

[2] C. Miehe, and F.. Welschinger and M. Hofacker, *Thermodynamically consistent phase-field models of fracture: Variational principles and multi-field FE implementations*, International journal for numerical methods in engineering **83** (2010), 1273–1311.

[3] F. Freddi, and G. Royer-Carfagni, *Variational fracture mechanics to model compressive splitting of masonry-like materials*, Annals of Solid and Structural Mechanics **2** (2011), 57–67.

[4] L. De Lorenzis, and C. Maurini, *Nucleation under multi-axial loading in variational phase-field models of brittle fracture*, International Journal of Fracture **237** (2022), 61–81.

Meshfree method applied to the dynamic fracture in quasi-brittle materials: an eigensoftening approach

Rena C Yu

(joint work with Pedro Navas, Bo Li, Gonzalo Ruiz)

In the realm of numerical modeling, our work with the eigensoftening algorithm marks a significant leap forward from the traditional eigenerosion approach, especially in the context of accurately capturing the nuances of material failure in concrete. The essence of eigensoftening lies in its refined mathematical and computational techniques, which are meticulously tailored to estimate tensile stresses and peak strains with remarkable precision. This advanced algorithm, with its intricate modifications, stands in closer alignment with experimental data, thereby offering a more realistic representation of material behavior under stress [1].

Delving into the experimental validation, the three-point bending tests conducted on concrete samples using a drop-weight device were meticulously designed. These tests, characterized by their detailed specifications such as the concrete sample dimensions and the precise calibration of the drop-weight, were augmented with strategically placed strain gauges to capture a comprehensive dataset. The comparison of these experimental results with the model predictions was not just a

matter of numerical matching; it involved sophisticated statistical analyses, highlighting how the eigensoftening algorithm significantly narrows down the error margins, offering a more robust and reliable prediction of material behavior.

In the realm of energy dissipation analysis, the eigensoftening algorithm sheds light on the intricate dynamics of energy evolution and distribution within concrete beams under varying impact speeds. This analysis reveals intriguing insights, particularly the observation that the area under the reaction-deflection curve vastly overshadows the energy dissipated due to fractures.

The foray into modeling fiber reinforced concrete using the eigensoftening algorithm is yet another testament to its versatility [2]. The adoption of a bilinear relation for this purpose marks a significant departure from the linear softening stress-equivalent crack opening relation, offering a more nuanced understanding of the dynamic fracture behavior of such materials. The influence of the notch position on crack patterns, a key finding from this study, opens up new avenues for material design, particularly in optimizing fiber reinforced concrete structures for enhanced durability and resilience.

Our parametric studies, exploring various notch positions, add another layer of depth to our understanding of concrete behavior. These studies are not confined to academic curiosity but are rooted in practical applications, potentially influencing the design of structures in seismically active regions.

Looking ahead, the potential applications of the eigensoftening algorithm extend beyond its current use. Its adaptability to different materials and loading conditions, coupled with the profound implications of our findings for industrial and real-world applications, suggest a future where this research could significantly influence construction practices and material selection.

References

[1] Navas, P., R. C. Yu, B. Li, and G. Ruiz, *Modeling the dynamic fracture in concrete: an eigensoftening meshfree approach*, International Journal of Impact Engineering **113** (2018), 9–20.

[2] Yu, R. C., P. Navas, and G. Ruiz, *Meshfree modeling of the dynamic mixed-mode fracture in FRC through an eigensoftening approach*, Engineering Structures, **172** (2018), 94–104.

Effective Models for Membranes and Plates with Soft Inclusions and an Eigendeformation Model for Cohesive Fracture

Bernd Schmidt

(joint work with V. Auer-Volkmann, L. Beck, M. Santilli)

We report on some recent results on effective theories and their approximation for objects that are subject to both elastic deformations and fracture. In part 1 we study the formation of voids and cracks in membranes and (Kirchhoff-)plates, [7, 8]. In part 2 we extend the Eigenfracture approximation for brittle materials [9] to materials undergoing cohesive fracture, [1, 2].

Part 1. Membranes and Plates with Soft Inclusions. We consider a reference configuration $\Omega \subset \mathbb{R}^3$ subject to the deformation $y \in W^{1,p}(\Omega, \mathbb{R}^3)$, $p \in (1, \infty)$, with an unknown 'void set' $D \in \mathcal{F}(\Omega)$ (a set of finite perimeter). Its configurational energy is assumed to be

$$\mathcal{E}(y, D) = \int_{\Omega \setminus D} W\big(\nabla y(x)\big)\, \mathrm{d}x + \int_{\Omega \cap \partial^* D} \psi\big(\nu(D)\big)\, \mathrm{d}\mathcal{H}^{n-1},$$

where W satisfies a standard two-sided L^p growth condition, ψ is a norm on $\mathbb{R}^3$ and $\nu(D)$ denotes the (exterior measure-theoretic) unit-normal of D. A theorem of Braides, Chambolle and Solci in (see [3] and a simplified proof in [7]) identifies the (L^1-)relaxation of $\mathcal{E}$ on $GSBV_1^p(\Omega; \mathbb{R}^m) \times \mathcal{F}(\Omega)$ in which W is replaced by its quasiconvex hull W^{qc} and an additional surface term on $J_y \cap D^0$, D^0 the measure theoretic exterior of D, with density ψ depending on the crack normal $\nu(y)$ occurs.

Our first objective is to extend this analysis to thin membranes. More precisely, we consider the same functional on the h-dependent domain $\Omega_h = \omega \times (0, h) \subset \mathbb{R}^3$, and seek to analyze its asymptotics as $h \searrow 0$. Rescaling the domain to $\Omega = \omega \times (0, 1)$ and the energy by h^{-1}, this amounts to identifying the Γ-limit of

$$\mathcal{E}_h(y, D) = \int_{\Omega \setminus D} W\big(\nabla' y, \tfrac{1}{h}\partial_3 y\big)\, \mathrm{d}x + \int_{\Omega \cap \partial^* D} \psi\big(\nu'(D), \tfrac{1}{h}\nu_3(D)\big)\, \mathrm{d}\mathcal{H}^2$$

for $(y, D) \in W^{1,p}(\Omega; \mathbb{R}^3) \times \mathcal{F}(\Omega)$.

To this end, we introduce x_3-relaxed densities $W_0(\xi') = \inf\big\{W(\xi', \xi_3) : \xi_3 \in \mathbb{R}^3\big\}$ for $\xi' \in \mathbb{R}^{3\times 2}$ and $\psi_0(\nu') = \inf\big\{\psi(\nu', \nu_3) : \nu_3 \in \mathbb{R}\big\}$ for $\nu' \in \mathbb{R}^2$.

Theorem A. The $\mathcal{E}_h$ $\Gamma(L^1)$-converge to $\mathcal{E}_0^{\mathrm{rel}} : GSBV_1^p(\omega; \mathbb{R}^3) \times \mathcal{F}(\omega) \to \mathbb{R}$, where

$$\begin{aligned}\mathcal{E}_0^{\mathrm{rel}}(y, D) = &\int_{\omega \setminus D} W_0^{\mathrm{qc}}(\nabla' y)\, \mathrm{d}x \\ &+ 2\int_{J_y \cap D^0} \psi_0(\nu'(y))\, \mathrm{d}\mathcal{H}^1 + \int_{\omega \cap \partial^* D} \psi_0(\nu'(D))\, \mathrm{d}\mathcal{H}^1.\end{aligned}$$

The proof of this theorem, together with a matching compactness result is contained in [7]. We also mention the related analysis provided in [4] for brittle membranes.

We now consider thin elastic plates whose stored energy functional is the same as for membranes, but whose fracture toughness scales with h^2. Rescaling their energy by h^{-3} now leads to

$$\mathcal{E}_h(y, D) = \frac{1}{h^2}\int_{\Omega \setminus D} W\big(\nabla' y, \tfrac{1}{h}\partial_3 y\big)\, \mathrm{d}x + \int_{\Omega \cap \partial^* D} \psi\big(\nu'(D), \tfrac{1}{h}\nu_3(D)\big)\, \mathrm{d}\mathcal{H}^2$$

for $(y, D) \in W^{1,p}(\Omega; \mathbb{R}^3) \times \mathcal{F}(\Omega)$. We assume suitable growth and smoothness assumptions on W and introduce an 'x_3-relaxed' Hessian Q_2 at Id on $\mathbb{R}^{2\times 2}$ and let ψ_0 as before. We define the space

$$\begin{aligned}SBV_{\mathrm{iso}}^{2,2}(\omega) = \big\{&r \in SBV^2(\omega, \mathbb{R}^3) \cap L^\infty(\omega, \mathbb{R}^3) : \\ &\nabla r \in SBV^2(\omega, \mathbb{R}^{3\times 2}), (\nabla r, \partial_1 r \wedge \partial_2 r) \in \mathrm{SO}(3) \text{ a.e.}\big\}\end{aligned}$$

and the second fundamental form of $r \in SBV^{2,2}_{\mathrm{iso}}(\omega)$ as

$$\mathrm{II}_r = -\big(\partial_{ij} r \cdot (\partial_1 r \wedge \partial_2 r)\big)_{1\le i,j\le 2}.$$

Our main result for plates is the following passage to a limiting 'Blake-Zisserman-Kirchhoff' plate functional.

Theorem B. Under a technical 'minimal droplet assumption' and assuming L^∞ bounds one has a variational convergence result of the $\mathcal{E}_h$ in the sense of Γ-convergence as $y_h \to r$, $\chi_{D_h} \to \chi_D$ in L^1 to the limiting functional

$$\begin{aligned}\mathcal{E}(r,D) = \frac{1}{24}\int_{\omega\setminus D} Q_2(\mathrm{II})\,\mathrm{d}x' \\ + 2\int_{J_{(r,\nabla r)}\cap D^0} \psi_0(\nu(J_{(r,\nabla r)}))\,\mathrm{d}\mathcal{H}^1 + \int_{\omega\cap\partial^* D}\psi_0(\nu(D))\,\mathrm{d}\mathcal{H}^1\end{aligned}$$

for $(r,D) \in SBV^{2,2}_{\mathrm{iso}}(\omega)\times\mathcal{F}(\omega)$ (and $+\infty$ elsewhere on $L^\infty(\Omega,\mathbb{R}^3)\times\mathcal{F}(\Omega)$).

For the precise statement, its proof, a related compactness result and further discussion we refer to [8].

Part 2. An Eigendeformation Model for Cohesive Fracture. We now consider numerical approximation schemes for fracture problems. Our main aim is to extend the 'eigenfracture scheme' for britte fracture developed in [9] (which itself was motivated by the classical Ambrosio-Tortorelli scheme and nonlocal approximations through convolution integrals) to models that allow for cohesive fracture. Concentrating on the linearized antiplane shear setting we consider $E_\varepsilon : L^1(\Omega)\times\mathcal{M}(\Omega)\to[0,\infty]$,

$$E_\varepsilon(u,\gamma) := \begin{cases} \int_\Omega |\nabla u - g|^2\,\mathrm{d}x & \text{if } u\in W^{1,1}(\Omega),\ \|u\|_{L^\infty}\le K,\\ +\frac{1}{\varepsilon}\int_\Omega f\big(\varepsilon \fint_{B_\varepsilon(x)\cap\Omega}|g|\,\mathrm{d}t\big)\,\mathrm{d}x & \text{and } \gamma = g\mathcal{L}^1,\ g\in L^1(\Omega),\\ \infty & \text{otherwise on } L^1(\Omega)\times\mathcal{M}(\Omega).\end{cases}$$

Our main result is the following.

Theorem C. E_ε Γ-converges (w.r.t. the strong $\times$ flat topology on $L^1\times\mathcal{M}$) to $E : L^1(\Omega)\times\mathcal{M}(\Omega)\to\mathbb{R}\cup\{\infty\}$,

$$E(u,\gamma) := \begin{cases} \int_\Omega |\nabla u - g|^2\,\mathrm{d}x + \frac{G_c}{2}\int_\Omega |g|\,\mathrm{d}x & \text{if } u\in BV(\Omega),\ \|u\|_{L^\infty}\le K,\\ \quad + \int_{J_u}\theta(|[u]|)\,\mathrm{d}\mathcal{H}^{d-1} & \quad \gamma = D^s u + g\mathcal{L}^1,\\ \quad + \frac{G_c}{2}|D^c u|(\Omega) & \quad \nabla u - g\in L^2(\Omega),\\ \infty & \text{otherwise on } L^1(\Omega)\times\mathcal{M}(\Omega),\end{cases}$$

where θ is explicitly given as

$$\theta(s) := 2\int_0^1 f\left(\frac{\omega_{d-1}}{\omega_d}|s|\Big(\sqrt{1-t^2}\Big)^{d-1}\right)\mathrm{d}t \quad \text{for all } s\in\mathbb{R}.$$

For the proof, a related compactness result and further discussion we refer to [1, 2]. Here we only mention that in the one-dimensional setting the results in [5, 6] can be adapted (see [1]), while the general case is more involved, see [2].

For the functionals with energetically optimal eigendeformations we have:

Corollary D. The $\tilde{E}_\varepsilon(u) := \inf_{\gamma\in\mathcal{M}} E_\varepsilon(u,\gamma) = \inf_{g\in L^1} E_\varepsilon(u, g\mathcal{L}^d)$ Γ-converge to

$$\begin{aligned}\tilde{E}(u) &:= \inf_{g\in L^1} E(u, D^s u + g\mathcal{L}^d)\\ &= \int_\Omega \psi(|\nabla u|)\,\mathrm{d}x + c_0|D^c u|(\Omega) + \int_{J_u} \theta([u])\,\mathrm{d}\mathcal{H}^{d-1}\end{aligned}$$

for $u \in BV(\Omega)$, $\|u\|_{L^\infty} \le K$, $\gamma = D^s u + g\mathcal{L}^d$, $\nabla u - g \in L^2(\Omega,\mathbb{R}^d)$, $+\infty$ otherwise, where $\psi(t) = t^2$ if $t < \frac{c_0}{2}$ and $\psi(t) = c_0 t - \frac{c_0^2}{4}$ if $t \ge \frac{c_0}{2}$.

References

[1] V. Auer-Volkmann, L. Beck and B. Schmidt, *Eigendamage: an eigendeformation model for the variational approximation of cohesive fracture—a one-dimensional case study*, Ann. Mat. Pura Appl. **201** (2022), 2161–2195.

[2] V. Auer-Volkmann, L. Beck and B. Schmidt, *Eigendamage: an eigendeformation model for the variational approximation of cohesive fracture—antiplane shear deformations*, In preparation (2024).

[3] A. Braides, A. Chambolle and M. Solci, *A relaxation result for energies defined on pairs set-function and applications*, ESAIM Control Optim. Calc. Var. **13** (2007), 717–734.

[4] A. Braides and I. Fonseca, *Brittle thin films*, Appl. Math. Optim. **44** (2001), 299–323.

[5] L. Lussardi, E. Vitali, *Non-local approximation of free-discontinuity functionals with linear growth: the one-dimensional case*, Ann. Mat. Pura Appl. **186** (2007), 721–744.

[6] L. Lussardi, E. Vitali, *Non-local approximation of free-discontinuity problems with linear growth*, ESAIM Control Optim. Calc. Var. **13** (2007), 135–162.

[7] M. Santilli and B. Schmidt, *Two-phase models for elastic membranes with soft inclusions*, Atti Accad. Naz. Lincei Rend. Lincei Mat. Appl. **34** (2023), 401–431.

[8] M. Santilli and B. Schmidt, *A Blake-Zisserman-Kirchhoff theory for plates with soft inclusions*, J. Math. Pures Appl. **175** (2023), 143–180.

[9] B. Schmidt, F. Fraternali and M. Ortiz, *Eigenfracture: an eigendeformation approach to variational fracture*, Multiscale Model. Simul. **7** (2008), 1237–1266.

Towards a Complete Theory of Fracture: The Insightful Case of Elastomers

Oscar Lopez-Pamies

In the first part of this talk, I will review what is that is known at present from centuries of experimental observations about the nucleation and propagation of fracture in elastomers subjected to mechanical loads applied monotonically and quasi-statically.

The observations will reveal that there are three basic ingredients that any attempt at a complete macroscopic theory of fracture ought to account for:

- the stored-energy function
$$W(\mathbf{F})$$
describing the elasticity of the elastomer for arbitrary deformation gradients $\mathbf{F}$,
- the strength surface
$$\mathcal{F}(\mathbf{S}) = 0$$
describing the strength of the elastomer for arbitrary first Piola–Kirchhoff stress tensors $\mathbf{S}$, and
- the critical energy release rate
$$G_c$$
describing the intrinsic fracture energy of the elastomer, that is, the amount of energy per unit undeformed area required to create new surface in the elastomer.

Having pinpointed the basic ingredients required for a complete theory, I will then present one such theory, regularized, of phase-field type for the basic case of nominally elastic brittle elastomers [1, 2, 3]. The theory can be viewed as a natural generalization of the phase-field approximation [4] of the celebrated variational theory of brittle fracture of Francfort and Marigo [5] — which is nothing more than the mathematical statement of Griffith's [6] competition of bulk and fracture energies in its general form — to account for the strength of the elastomer.

In the second part of the talk, I will deploy the theory in order to explain in a detailed and quantitative manner the nucleation and propagation of fracture in poker-chip experiments, both on natural rubber [7, 8] and on synthetic elastomers [9, 10]. In a nutshell, the simulations will show that

(1) The nucleation of internal cracks in poker-chip experiments of elastomers is dominated by the strength — in particular, the entire first octant $\mathbf{S} = \mathrm{diag}(s_1 > 0, s_2 > 0, s_3 > 0)$ of the strength surface $\mathcal{F}(\mathbf{S}) = 0$ — of the elastomer. That is, internal cracks nucleate in regions where the strength surface of the elastomer has been exceeded, soon after it has been exceeded.
(2) For an elastomer whose hydrostatic strength $s_{\mathtt{hs}}$ is comparable to or smaller than its uniaxial $s_{\mathtt{ts}}$ and biaxial $s_{\mathtt{bs}}$ tensile strengths, the first nucleation of internal cracks occurs around the centerline of the specimen.
(3) For an elastomer whose hydrostatic strength $s_{\mathtt{hs}}$ is large relative to its uniaxial $s_{\mathtt{ts}}$ and biaxial $s_{\mathtt{bs}}$ tensile strengths, the first nucleation of internal cracks occurs radially away from the centerline of the specimen.
(4) If in addition to featuring a relatively large hydrostatic strength, the elastomer features a relatively small critical energy release rate G_c, the first nucleation of cracks occurs from the free boundary of the specimen near one of the fixtures. In this case, the nucleated cracks are *not* internal but external cracks.
(5) The propagation of all nucleated (internal and external) cracks is governed by the Griffith competition between the bulk elastic energy of the synthetic

elastomer and its constant intrinsic fracture energy. This competition leads to the nucleation of fewer internal cracks in thicker specimens.

These findings provide a complete description and explanation of the poker-chip experiments of elastomers at large and thus bring resolution to the understanding of one of the pioneering problems in the fracture of soft matter, one that had remained open for over six decades.

What is more, the results provide compelling evidence that the proposed theory may indeed provide a complete framework for the description of fracture nucleation and propagation in elastic brittle materials at large — not just elastomers — under arbitrary monotonic and quasi-static loadings.

References

[1] Kumar, A., Francfort, G.A., Lopez-Pamies, O., *Fracture and healing of elastomers: A phase-transition theory and numerical implementation*, J. Mech. Phys. Solids **112** (2018), 523–551.

[2] Kumar, A., Lopez-Pamies, O., *The phase-field approach to self-healable fracture of elastomers: A model accounting for fracture nucleation at large, with application to a class of conspicuous experiments*, Theor. Appl. Fract. Mech. **107** (2020), 102550.

[3] Kumar, A., Bourdin, B., Francfort, G.A., Lopez-Pamies, O., *Revisiting nucleation in the phase-field approach to brittle fracture*, J. Mech. Phys. Solids **142** (2020), 104027.

[4] Bourdin, B., Francfort, G.A., Marigo, J.J., *Numerical experiments in revisited brittle fracture*, J. Mech. Phys. Solids **48** (2000), 797–826.

[5] Francfort, G.A., Marigo, J.J., *Revisiting brittle fracture as an energy minimization problem*, J. Mech. Phys. Solids **46** (1998), 1319–1342.

[6] Griffith, A.A., *The phenomena of rupture and flow in solids*, Philos. Trans. R. Soc. Lond. A **221** (1921), 163–198.

[7] Gent, A.N., Lindley, P.B., *Internal rupture of bonded rubber cylinders in tension*. Proc. R. Soc. Lond. Ser. A Math. Phys. Eng. Sci. **249**, 195–205.

[8] Kumar, A., Lopez-Pamies, O., *The poker-chip experiments of Gent and Lindley (1959) explained*, J. Mech. Phys. Solids **150** (2021), 104359.

[9] Guo, J., Ravi-Chandar, K., *On crack nucleation and propagation in elastomers: I. In situ optical and X-ray experimental observations*, Int. J. Fract. **243** (2024), 1–29.

[10] Kamarei, F., Kumar, A., Lopez-Pamies, O., *The poker-chip experiments of synthetic elastomers*, Submitted (2024).

Nonlocal curvature for integrable interaction kernels

Petronela Radu

(joint work with Animesh Biswas, Mikil Foss)

Curvature is a fundamental concept in physics and it plays a crucial role in various areas such as: classical mechanics, general relativity, optics, and fluid dynamics. In particular, the curvature of surfaces can affect the mechanical, electrical, and optical properties of materials, so curvature effects need to be taken into account when designing and analyzing new materials. The recently introduced concept of nonlocal curvatures provide a frameworks for measuring the "bend" of a surface under little or no smoothness assumptions, while connecting to classical curvature as the horizon of interaction converges to zero.

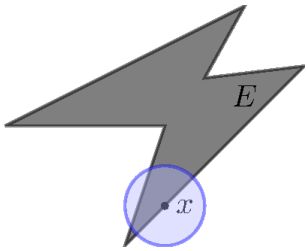

This talk focuses on the problem of constant nonlocal curvature defined via integrable kernel. Our results offer some extensions to the constant mean curvature problem for nonintegrable kernels, where counterparts to Alexandrov theorem [1] in the nonlocal framework were established independently by two separate groups. Ciraolo, Figalli, Maggi, Novaga [4] and respectively, Cabré, Fall, Solà-Morales, Weth [2, 3]. Using the nonlocal version of Alexandrov's moving plan method, we identify surfaces of constant nonlocal mean curvature based on integrable kernels and show they are unions of balls situated at distance $\delta > 0$ apart, where δ measures the radius of nonlocal interactions.

In the second part of this talk we will present some results related to the concept of *ordered curvature*. In the classical setting, Li and Nirenberg studied the problem where the mean curvature is assumed to be monotone (ordered) in a given direction ν. Under certain geometric assumptions, they showed that there must be a hyperplane orthogonal to ν across which the surface is symmetric. Thus, if the mean curvature is ordered in all directions, the surface is a sphere. we have developed the concept of nonlocal ordered curvature, but considering the nonlocal curvature for a surface of minimal regularity (for example, open sets) under some technical, but general assumptions regarding intersections of the set with parallel lines.

Given a measurable set $\Omega \subseteq \mathbb{R}^n$, the nonlocal curvature at $x \in \mathbb{R}^n$ associated with an integrable kernel J, is defined as

$$H^J_\Omega(x) := \int_{\mathbb{R}^n} J(x-y)(\chi_\Omega(y) - \chi_{\Omega^c}(y)) = \int_{\mathbb{R}^n} J(x-y)\tau_\Omega(y)dy,$$

where χ_Ω is the characteristic function of the set Ω. When J is the characteristic function of a ball of radius r (i.e. $J(x-y) = 1$ for $|x-y| < r$ and $J(x-y) = 0$, otherwise) the curvature simply measures the difference between the volume of the set Ω inside the ball and the volume outside the ball - see figure below. While the concept is easily formulated, the computation of nonlocal curvature, even for sets with polygonal contours, is non-trivial. Similarly, the theoretical analysis requires careful estimates. Yet, the physical motivation and intuition behind its definition propels it as an important and efficient tool in applications.

References

[1] D. Alexandrov, *Uniqueness theorems for surfaces in the large ν*, Vestnik Leningrad Univ. **19**, (1958), 5–8.

[2] X. Cabré, M. Fall, J. Sola-Morales, T. Weth, *Curves and surfaces with constant nonlocal mean curvature: meeting Alexandrov and Delaunay*, J. Reine Angew. Math., (2018), 253–280.

[3] X. Cabré, M. Fall, T. Weth, Near-sphere lattices with constant nonlocal mean curvature, Mathematische Annalen, **370**, (2018), 1513–1569.

[4] G. Ciraolo, A. Figalli, F. Maggi, M. Novaga, *Rigidity and sharp stability estimates for hypersurfaces with constant and almost-constant nonlocal mean curvature*, J. Reine Angew. Math., (2018), 275–294.

Phase-field fracture in finitely-strained viscoelastic solids in an Eulerian formulation

Tomáš Roubíček

Continuum mechanics and thermomechanics of solids at finite strains can be formulated either in the referential frame (i.e. the Lagrangian approach) or in the actual evolving frame (i.e. the Eulerian approach). Of course, these options apply also to the damage mechanics. Here the latter option is considered.

The basic kinematic ingredients are the Eulerian velocity $\boldsymbol{v}$ and the deformation gradient $\boldsymbol{F}$, subjected to the evolution rule $\dot{\boldsymbol{F}}=(\nabla\boldsymbol{v})\boldsymbol{F}$ where the dot denotes the convective time derivative, i.e. $\dot{\boldsymbol{F}}=\frac{\partial}{\partial t}\boldsymbol{F}+(\boldsymbol{v}\cdot\nabla)\boldsymbol{F}$. Beside the usual Kelvin-Voigt rheology, one can consider rheologies with internal variables. The simplest one is of the Maxwell type (describing creep or plasticity) using the Kröner-Lee-Liu multiplicative decomposition $\boldsymbol{F}=\boldsymbol{F}_{\rm e}\boldsymbol{F}_{\rm p}$ to the elastic and the inelastic distortions $\boldsymbol{F}_{\rm e}$ and $\boldsymbol{F}_{\rm p}$, combined possibly with the Stokes' type viscosity. Introducing the inelastic distortion rate $\boldsymbol{L}_{\rm p}=\dot{\boldsymbol{F}}_{\rm p}\,\boldsymbol{F}_{\rm p}^{-1}$, one can eliminate $\boldsymbol{F}$ and $\boldsymbol{F}_{\rm p}$, obtaining the kinematic equation for $\boldsymbol{F}_{\rm e}$ as $\dot{\boldsymbol{F}}_{\rm e}=(\nabla\boldsymbol{v})\boldsymbol{F}_{\rm e}-\boldsymbol{F}_{\rm e}\boldsymbol{L}_{\rm p}$.

This basic kinematics is then used for visco-elastodynamics considered mostly within a framework of hyperelastic materials, i.e. the symmetric Cauchy stress is derived from a stored energy $\varphi=\varphi(\boldsymbol{F}_{\rm e})$. In principle, there are three options how to understand φ: as a referential potential in Pa (as energy per referential volume) or as an actual potential in Pa (as energy per actual current volume) or as a referential potential in J/kg as energy per mass, to which the corresponding Cauchy stress $\boldsymbol{T}$ is $\varphi'(\boldsymbol{F}_{\rm e})\boldsymbol{F}_{\rm e}^{\top}/\det\boldsymbol{F}_{\rm e}$ or $\varphi'(\boldsymbol{F}_{\rm e})\boldsymbol{F}_{\rm e}^{\top}+\varphi(\boldsymbol{F}_{\rm e})\mathbb{I}$ or $\varrho\varphi'(\boldsymbol{F}_{\rm e})\boldsymbol{F}_{\rm e}^{\top}$ with ϱ denoting the mass density, respectively. Below in (2), we will choose the 2nd one.

This basic isothermal scenario can be then enhanced by considering varying temperature θ or/and various internal variables like damage (or phase field) denoted by α, or porosity, aging, or some fluid content, etc. Depending on θ, one should speak rather about free energy ψ than mere stored energy φ. Here, one should think about letting $\psi=\psi(\boldsymbol{F}_{\rm e},\alpha,\theta)$.

The full thermodynamically consistent model should then comply with the 2nd-law of thermodynamics (expressed by Clausius-Duhem inequality) through the

entropy equation

$$\dot\eta = \frac{\xi - \operatorname{div}\boldsymbol{j}}{\theta} - (\operatorname{div}\boldsymbol{v})\eta\,, \tag{1}$$

where $\eta = -\psi_\theta(\boldsymbol{F}_{\rm e},\alpha,\theta)$ denotes the entropy, ξ denotes the dissipation rate, and $\boldsymbol{j}$ denotes the heat flux considered governed by the Fourier law (in the physical form) as $\kappa\nabla(1/\theta)$ with $\kappa=\kappa(\theta)$ denoting a (rescaled) heat conductivity coefficient. From (1), one obtains the heat equation, cf. (2f) below.

Other ingredients are dissipation potentials: $\zeta=\zeta(\theta;\boldsymbol{e}(\boldsymbol{v}))$ for the Stokes viscosity with $\boldsymbol{e}(\boldsymbol{v})=\frac12\nabla\boldsymbol{v}^\top+\frac12\nabla\boldsymbol{v}$, $\zeta_{\rm p}=\zeta_{\rm p}(\theta;\boldsymbol{L}_{\rm p})$ for the inelastic distortion (plasticity or Maxwellian creep), and $\zeta_{\rm d}=\zeta_{\rm d}(\theta;\dot\alpha)$ for the damage (or a phase-field).

We consider (as most often) the isochoric inelastic distortion, i.e. $\det\boldsymbol{F}_{\rm p}=1$. Thermodynamically coupled system for the six-tuple $(\varrho,\boldsymbol{v},\boldsymbol{F}_{\rm e},\boldsymbol{L}_{\rm p},\alpha,\theta)$ consists from the continuity equation for the mass density, the momentum equation, the mentioned kinematic equation for $\boldsymbol{F}_{\rm e}$, a flow rule for the inelastic distortion, a flow rule for damage α, and a heat-transfer equation for temperature θ:

$$\dot\varrho = -\varrho\operatorname{div}\boldsymbol{v}\,, \tag{2a}$$

$$\varrho\dot{\boldsymbol{v}} = \operatorname{div}(\boldsymbol{T}+\boldsymbol{D}+\boldsymbol{K})+\varrho\boldsymbol{g},\quad \text{with}\ \ \boldsymbol{T}=\boldsymbol{S}\boldsymbol{F}_{\rm e}^\top+\psi(\boldsymbol{F}_{\rm e},\alpha,\theta)\mathbb{I}\,, \tag{2b}$$
$$\boldsymbol{D}=\zeta'_{\boldsymbol{e}}(\theta;\boldsymbol{e}(\boldsymbol{v}))-\operatorname{div}(\nu(\theta)|\nabla^2\boldsymbol{v}|^{p-2}\nabla^2\boldsymbol{v})\,,$$
$$\boldsymbol{K}=\mu\nabla\alpha\otimes\nabla\alpha-\frac{\mu}{2}|\nabla\alpha|^2\mathbb{I},\ \ \text{and}\ \ \boldsymbol{S}=\psi'_{\boldsymbol{F}_{\rm e}}(\boldsymbol{F}_{\rm e},\alpha,\theta)\,,$$

$$\dot{\boldsymbol{F}}_{\rm e}=(\nabla\boldsymbol{v})\boldsymbol{F}_{\rm e}-\boldsymbol{F}_{\rm e}\boldsymbol{L}_{\rm p}\,, \tag{2c}$$

$$\partial_{\boldsymbol{L}_{\rm p}}\zeta_{\rm p}(\theta;\boldsymbol{L}_{\rm p})\ni-\operatorname{dev}(\boldsymbol{F}_{\rm e}^\top\boldsymbol{S})+\operatorname{div}(\kappa_{\rm p}(\theta)|\nabla\boldsymbol{L}_{\rm p}|^{q-2}\nabla\boldsymbol{L}_{\rm p})\,, \tag{2d}$$

$$\partial_{\dot\alpha}\zeta_{\rm d}(\theta;\dot\alpha)\ni\mu\Delta\alpha-\psi'_\alpha(\boldsymbol{F}_{\rm e},\alpha,\theta)\,, \tag{2e}$$

$$\dot w=\xi(\alpha;\nabla\boldsymbol{v},\boldsymbol{L}_{\rm p},\dot\alpha)-\operatorname{div}\boldsymbol{j}+\psi'_{\boldsymbol{F}_{\rm e}}(\boldsymbol{F}_{\rm e},\alpha,\theta)\!:\!\dot{\boldsymbol{F}}_{\rm e}+\big(\psi(\boldsymbol{F}_{\rm e},\alpha,\theta)-w\boldsymbol{v}\big)\operatorname{div}\boldsymbol{v} \tag{2f}$$
$$\text{with}\ \ w=\omega(\boldsymbol{F}_{\rm e},\alpha,\theta):=\psi(\boldsymbol{F}_{\rm e},\alpha,\theta)-\theta\psi'_\theta(\boldsymbol{F}_{\rm e},\alpha,\theta)\,,\quad \boldsymbol{j}=\kappa(\theta)\nabla\frac{1}{\theta}\,,$$
$$\text{and}\ \xi(\alpha;\nabla\boldsymbol{v},\boldsymbol{L}_{\rm p},\dot\alpha)=\zeta'_{\boldsymbol{e}}(\theta;\boldsymbol{e}(\boldsymbol{v}))\!:\!\boldsymbol{e}(\boldsymbol{v})+\partial_{\boldsymbol{L}_{\rm p}}\zeta_{\rm p}(\theta;\boldsymbol{L}_{\rm p})\!:\!\boldsymbol{L}_{\rm p}$$
$$+\nu(\theta)|\nabla^2\boldsymbol{v}|^p+\kappa_{\rm p}(\theta)|\nabla\boldsymbol{L}_{\rm p}|^2+\dot\alpha\,\partial_{\dot\alpha}\zeta_{\rm d}(\theta;\dot\alpha).$$

The variable $w=\psi+\theta\eta$ in (2f) is the internal energy while $\boldsymbol{F}_{\rm e}^\top\boldsymbol{S}$ in (2d) is (the deviatoric part of) the Mandel stress. The higher-order contribution to the dissipative contribution $\boldsymbol{D}$ to the Cauchy stress in (2b) which involves the "hyperstress" $\nu(\theta)|\nabla^2\boldsymbol{v}|^{p-2}\nabla^2\boldsymbol{v}$ is known as a concept of the so-called 2nd-grade multipolar (nonsimple) materials. Analytically, for p bigger than space dimension, this term ensures Lipschitz continuity of the velocity field $\boldsymbol{v}$ in space, which in turn avoids developing of singularities in the transport equations (2a) and (2c), cf. [3, 4, 6, 7].

The system is to be completed by suitable (here unspecified) boundary conditions. Let us only say that, in the Eulerian formulation, the most often one imposes the impenetrability condition $\boldsymbol{v}\cdot\boldsymbol{n}=0$ with $\boldsymbol{n}$ denoting the normal to the boundary of a domain Ω on which the system (2) is considered.

The energetics behind the system is revealed when testing (2b) by $\boldsymbol{v}$, (2d) by $\boldsymbol{L}_{\rm p}$, (2e) by $\dot\alpha$, and (2f) by 1. After some calculations within which we used also (2a) tested by $\frac12|\boldsymbol{v}|^2$ and (2c) tested by ψ, we obtain a balance for the total (i.e.

kinetic and internal) energy:

$$\frac{\mathrm{d}}{\mathrm{d}t}\int_\Omega \frac{\varrho}{2}|\boldsymbol{v}|^2+\omega(\boldsymbol{F}_{\rm e},\alpha,\theta)+\frac{\mu}{2}|\nabla\alpha|^2\,\mathrm{d}\boldsymbol{x}=\int_\Omega \varrho\boldsymbol{g}\cdot\boldsymbol{v}\,\mathrm{d}\boldsymbol{x}\,, \tag{3}$$

which expresses the 1st law of thermodynamics. The symmetric Korteweg-type stress $\boldsymbol{K}$ in (2b) balances the energy when confronted by the term $\mu\Delta\alpha$ in (2e) tested by the convective derivative $\dot\alpha$. Also the expected entropy balance complying with the Clausius-Duhem inequality (the 2nd law of thermodynamics) is fulfilled.

It should be emphasized that the Korteweg stress $\boldsymbol{K}$ is related with the Eulerian formulation of the gradient damage and, depending nonlinearly on $\nabla\alpha$, needs strong convergence of $\nabla\alpha$ of the (here unspecified) approximate solutions. This causes specific analytical problems which seem ultimately to require $\zeta_{\rm d}(\theta;\cdot)$ with a polynomial growth, i.e. to allow damage healing. The unidirectional damage in Eulerian formulation thus seems analytical as an open problem.

An example of a referential free energy $\psi_{\rm R}$ is a neo-Hookean model with a volumetric-deviatoric split allowing for modelling of a mode-dependent fracture distinguishing pressure vs tension in Mode I, with a damageable bulk elastic modulus $K_{\rm E}$ and a damageable shear elastic modulus $G_{\rm E}$, combined with the phase-field fracture with $G_{\rm c}>0$ a fracture toughness and $\varepsilon>0$ a regularizing parameter, $\theta_0>0$ a reference temperature at which the heat capacity is c_0, and $\gamma>0$:

$$\begin{aligned}\psi_{\rm R}(\boldsymbol{F}_{\rm e},\alpha,\theta)=\frac{1}{2}K_{\rm E}(\alpha)\big([\det\boldsymbol{F}_{\rm e}{-}1]^+\big)^2+\frac{1}{2}K_{\rm E}(0)\big([\det\boldsymbol{F}_{\rm e}{-}1]^+\big)^2\\ +G_{\rm E}(\alpha)\frac{\mathrm{tr}(\boldsymbol{F}_{\rm e}\boldsymbol{F}_{\rm e}^\top)}{(\det\boldsymbol{F}_{\rm e})^{2/d}}+\frac{G_{\rm c}\det\boldsymbol{F}_{\rm e}}{2\varepsilon}\alpha^2-\frac{c_0\theta^{1+\gamma}}{\gamma(1{+}\gamma)\theta_0^\gamma}\,.\end{aligned} \tag{4}$$

The actual free energy ψ which would then be used for (2) is then $\psi(\boldsymbol{F}_{\rm e},\alpha,\nabla\alpha,\theta)=\psi_{\rm R}(\boldsymbol{F}_{\rm e},\alpha,\nabla\alpha,\theta)/\det\boldsymbol{F}_{\rm e}$. The actual heat capacity $c(\boldsymbol{F}_{\rm e},\theta)=-\theta\psi''_{\theta\theta}(\boldsymbol{F}_{\rm e},\theta)$ is then $c_0(\theta/\theta_0)^\gamma/\det\boldsymbol{F}_{\rm e}$ and satisfies $c(\boldsymbol{F}_{\rm e},0)=0$, which is the physically relevant attribute advocated already by W. Nernst. Combining it with the $\nabla\alpha$-term with $\mu=G_{\rm c}\varepsilon$, we obtain the Ambrosio-Tortorelli phase-field fracture model.

The model (2) is very general with a lot of potential applications. Particular cases are modeling of rupture of tectonic faults with earthquakes or a birth of new faults or fracture combined with a thermomechanical Stefan-type phase transition with a latent heat and melting/healing (as in ice/water or in rock/magma). A benefit from the Eulerian formulation is a possibility of direct coupling with spatial fields as gravitational or electromagnetic, or of coupling of solids and fluids.

Acknowledgment: This research was done under the grants 22-00863K "Controllable metamaterials and smart structures: nonlinear problems, modelling and experiments" of the Czech Sci. Foundation.

References

[1] T. Roubíček, *Models of dynamic damage and phase-field fracture, and their various time discretisations*. In: *Topics in Applied Analysis and Optimisation* (Eds. J.-F. Rodrigues and M. Hintermüller) Springer, 2019, pp.363–396.

[2] T. Roubíček, *Thermodynamically consistent model for poroelastic rocks towards tectonic and volcanic processes and earthquakes*, Geophysical J. Intl., **227** (2021), 1893–1904.

[3] T. Roubíček, *Visco-elastodynamics at large strains Eulerian*, Zeitschrift f. angew. Math. Phys., **73** (2022), art.no.80.
[4] T. Roubíček, *Quasistatic hypoplasticity at large strains Eulerian*, J. Nonlin. Sci., **32** (2022), Art.no.45.
[5] T. Roubíček, *The Stefan problem in a thermomechanical context with fracture and fluid flow*, Math. Math. Appl. Sci., **46** (2023), 12217–12245.
[6] T. Roubíček, *Interaction of finitely-strained viscoelastic multipolar solids and fluids by an Eulerian approach*, J. Math. Fluid Mech., **25** (2023), Art.no.22.
[7] T. Roubíček & G. Tomassetti, *Inhomogeneous finitely-strained thermoplasticity with hardening by an Eulerian approach*, Discrete Cont. Dynam. Systems – S, **17** (2024), 181–220.
[8] T. Roubíček & R.Vodička, *A monolithic model for phase-field fracture and waves in solid-fluid media towards earthquakes*, Intl. J. Fracture **219** (2019), 135–152, 2019.

Space-time phase-field fracture complementarity model and optimal control

Denis Khimin (Phd student talk)

In this talk we formulate a space-time continuous phase-field fracture model as an abstract energy minimization problem in a Banach space. First, optimality conditions for such a formulation, with a focus on the specific choice of function spaces to ensure the required regularity, are derived. Then, using the previously formulated optimality conditions, we present a higher level optimal control problem with constraints. Finally optimality conditions for the optimal control problem are stated.

Energy release rate and Griffith's criterion for phase field fracture

Matteo Negri
(joint work with Eleonora Maggiorelli)

Griffith's criterion [1] is widely used to model the propagation of sharp cracks in brittle materials: it is a rate independent criterion, usually written in Karush-Kuhn-Tucker form, based on the interplay between toughness $G_c > 0$ and energy release $G \geq 0$.

In the phase field context rate-independent evolutions are often obtained by means of time discrete schemes, providing (or selecting) at each time step an equilibrium configuration of the system. In practice, equilibria are computed by descent methods for the free energy (e.g., staggered and monolithic schemes) endowed with a suitable irreversibility constraint on phase-field parameter (e.g., by monotonicity in time). Specifically, we consider [2] phase field energies of the form $\mathcal{F}(t,u,v) = \mathcal{E}(t,u,v) + G_c\mathcal{L}(v)$ where (for $\epsilon \ll 1$, $\eta = o(\epsilon)$, and $\delta = o(\epsilon)$)

$$\mathcal{E}(t,u,v) = t^2 \int_\Omega W_{\rm el}(v,\boldsymbol{\varepsilon})\,dx, \quad W_{\rm el}(v,\boldsymbol{\varepsilon}) = \tfrac{1}{2}(v^2+\eta)\Big(|\boldsymbol{\varepsilon}_{\rm dev}|^2+|\boldsymbol{\varepsilon}^+_{\rm vol}|^2\Big)+|\boldsymbol{\varepsilon}^-_{\rm vol}|^2+\delta v^2,$$

$$\mathcal{L}(v) = \int_\Omega \epsilon^{-1}(v-1)^2 + \epsilon|\nabla v|^2\,dx,$$

We consider incremental problems in which at each time $t_k = k\tau$ the configuration is a separate minimizer of the energy $\mathcal{F}$, i.e.,

$$\begin{cases} u_{k+1} \in \operatorname{argmin}\{\mathcal{F}(t_{k+1}\,, u\,, v_{k+1}) \text{ for } u = tg \text{ on } \partial_D\Omega\} \\ v_{k+1} \in \operatorname{argmin}\{\mathcal{F}(t_{k+1}\,, u_{k+1}\,, v\,) \text{ for } v \le v(t_k)\}, \end{cases}$$

where the monotonicity constraint in v models irreversibility. In this way we provide a general result, which holds independently of the incremental scheme, since the update (u_{k+1}, v_{k+1}) could be a global minimizer, a local minimizer or simply a separate minimizer. In practice, numerical schemes employ energy descent algorithms, e.g. staggered [3], monolithic [4], active set [6] etc. converging (up to subsequences) to a separate minimizer of the energy.

Clearly, these time discrete evolutions are considered as approximations of their time continuous limit, to be computed as the time step vanishes. To this end we consider the affine interpolation v_τ of the time discrete configurations v_k. Compactness of v_τ is quite delicate since the limit evolution v is in general discontinuous in time. Technically, compactness relies on Kuratowski convergence of a suitable reparametrization of the time discrete points t_k, weak compactness of reparametrized evolutions, and on strong (a.e. in time) convergence of v_τ. Qualitatively, continuity points corresponds to the steady-sate regime while discontinuity points corresponds to the unsteady regime.

We provide [2] a few characterizations of the limit evolution v in the steady-state regime. The first is a variational system of the form

$$\begin{cases} \partial_u \mathcal{F}(t, u(t), v(t))[\phi] = 0 \quad \text{for every } \phi = 0 \text{ on } \partial_D\Omega, \\ \partial_v \mathcal{F}(t, u(t), v(t))[\xi] \ge 0 \quad \text{for every } \xi \le 0, \\ \partial_v \mathcal{F}(t, u(t), v(t))[\dot v(t)] = 0, \end{cases}$$

which holds a.e. in time. The second is the system of PDEs (actually, a weak variational inequality) which is of the form [6]

$$\begin{cases} \operatorname{div}(\boldsymbol{\sigma}(t)) = 0 & \Omega \\ \boldsymbol{\sigma}(t)\hat n = 0 & \partial_N\Omega \\ u(t) = tg & \partial_D\Omega, \end{cases}$$

$$\begin{cases} -\epsilon\Delta v(t) + \epsilon^{-1}(v(t) - 1) + \partial_v W_{\mathrm{el}}(v(t), \boldsymbol{\varepsilon}(t)) \le 0 & \text{in } \Omega \\ \partial_{\hat n} v(t) \le 0 & \text{on } \partial\Omega \\ \big[-\epsilon\Delta v(t) + \epsilon^{-1}(v(t) - 1) + \partial_v W_{\mathrm{el}}(v(t), \boldsymbol{\varepsilon}(t)) \big]\, \dot v(t) = 0 & \text{in } \Omega \\ \partial_{\hat n} v(t)\, \dot v(t) = 0 & \text{on } \partial\Omega, \end{cases}$$

and holds in the sense of measures, under the regularity assumption $\dot v(t) \in C(\bar\Omega)$.

Moreover, as far as properties, we show that the monotonicity constraint turns out to be thermodynamically consistent since the dissipated energy is monotone

in time, i.e. $\partial_v \mathcal{L}(v(t))[\dot{v}(t)] \geq 0$, and since $\partial_v \mathcal{L}(v(t))[\xi] > 0$ for every $\xi \leq 0$ with $\xi \neq 0$.

Finally, we provide a characterization of the evolution in terms of Griffith's criterion. To this end we first define the energy release [7] to be given by

$$\mathcal{G}(t,v) = \sup\{-\partial_v \tilde{\mathcal{E}}(t,v)[\xi] : \xi \leq 0 \text{ with } d\mathcal{L}(v)[\xi] = 1\}$$

where $\tilde{\mathcal{E}}(t,v) = \mathcal{E}(t,u_{t,v},v)$ and $u_{t,v} \in \operatorname{argmin}\{\mathcal{E}(t,u,v) : u = tg \text{ on } \partial_D\Omega\}$. In equilibrium points, we actually have [2]

$$\mathcal{G}(t,v) = \limsup_{z \nearrow v} -\frac{\tilde{\mathcal{E}}(t,z) - \tilde{\mathcal{E}}(t,v)}{\mathcal{L}(z) - \mathcal{L}(v)} = \max\left\{-\frac{d\tilde{\mathcal{E}}(t,v)[\xi]}{d\mathcal{L}(v)[\xi]} : \xi \leq 0 \text{ and } \xi \neq 0\right\}.$$

The limit evolution v satisfies Griffith's criterion, in the following form. In the steady state regime, for a.e. $t \in [0,T]$ we have

$$\begin{cases} \dot{v}(t) \leq 0 \text{ and } \dot{\mathcal{L}}(t) = d\mathcal{L}(v(t))[\dot{v}(t)] \geq 0 \\ \mathcal{G}(t,v(t)) \leq G_c \\ (\mathcal{G}(t,v(t)) - G_c)\,\dot{\mathcal{L}}(t) = 0 \\ \mathcal{G}(t,v(t)) = -\partial_v \tilde{\mathcal{E}}(t,v(t))[\lambda\dot{v}(t)] \text{ where } d\mathcal{L}(v(t))[\lambda\dot{v}(t)] = 1. \end{cases}$$

In the unstable (snap-back) regime: for every $t \in J_v$ we have

$$\begin{cases} v^+(t) \leq v^-(t) \text{ and } \mathcal{L}(v^+(t)) \geq \mathcal{L}(v^-(t)) \\ \mathcal{G}(t,v) \geq G_c \text{ for some } v \in \operatorname{co}\{v^-(t), v^+(t)\}. \end{cases}$$

Finally, we show that the limit v satisfies the energy identity

$$\begin{aligned} \mathcal{E}(t,u(t),v(t)) = \mathcal{E}(0,u_0,v_0) \; &+ \int_0^t \mathcal{P}_{ext}(t,u(t),v(t))\,dt \\ &- G_c\big(\mathcal{L}(v(t)) - \mathcal{L}(v_0)\big) + \sum_{t \in J_v} [\mathcal{F}(t,u(t),v(t))\,] \end{aligned}$$

where the jump $[\mathcal{F}(t,u(t),v(t))\,]$ is non-positive. We remark that in general there is no uniqueness of solutions.

Numerically, we compare the evolutions computed in the sharp crack setting using Griffith's criterion and in the phase field setting using an alternate minimization scheme, and thus satisfying the phase field Griffith's criterion stated above [2]. We consider in particular a couple of examples: a double cantilever beam and a single edge notch under tension. The first yields a steady state evolution, while the second gives an unstable discontinuous evolution concentrated in a single jump. The comparison (in terms of energy, energy release and evolution) shows a perfect consistency of the two approaches for the double cantilever beam and a very good consistency for the single edge notch under tension [8].

References

[1] A.A. Griffith, *The phenomena of rupture and flow in solids*, Phil. Trans. Roy. Soc. London **18** (1920), 163–198.

[2] E. Maggiorelli, M. Negri, *Energy release and Griffith's criterion for phase-field fracture*, in preparation.

[3] B. Bourdin, G. A. Francfort, and J.-J. Marigo, *Numerical experiments in revisited brittle fracture*, J. Mech. Phys. Solids **48** (200) 797–826.

[4] P. Farrell, C. Maurini, *Linear and nonlinear solvers for variational phase-field models of brittle fracture*, Int. J. Numer. Meth. Eng. **109** (2017) 648–667

[5] T. Heister, M. F. Wheeler, T. Wick, *A primal-dual active set method and predictor-corrector mesh adaptivity for computing fracture propagation using a phase-field approach*, Comp. Methods Applied Mech. Eng. **290** (2015) 466–495.

[6] T. Wick, *Multiphysics phase-field fracture*, Radon Series on Computational and Applied Mathematics **28** De Gruyter, Berlin (2020)

[7] D. Knees, M. Negri, *Convergence of alternate minimization schemes for phase field fracture and damage*, Math. Models Methods Appl. Sci. **27** (2017) 1743–1794.

[8] E. Maggiorelli, *Griffith criterion for steady and unsteady state crack propagation*, in preparation.

Phase-field modeling and computation of fatigue fracture

Pietro Carrara

(joint work with Jonas Heinzmann, Laura De Lorenzis)

The phase-field approach to fracture [1] is able to model crack nucleation and propagation by describing a steep but smooth transition from intact to fully cracked material states through a phase-field variable d [1]. In this context, the free energy of a linear elastic body occupying the domain Ω and susceptible of brittle fracture is written as

$$E_\ell(\boldsymbol{u}, d) = \int_\Omega \psi_{el}\left(\boldsymbol{\varepsilon}(\boldsymbol{u}), d\right) d\boldsymbol{x} + \frac{G_c}{4c_w}\int_\Omega \left(\frac{w(d)}{\ell} + \ell|\nabla d|^2\right) d\boldsymbol{x}\,. \tag{1}$$

where $\boldsymbol{x}$ is the spatial coordinate, $\boldsymbol{\varepsilon}(\boldsymbol{u})$ is the infinitesimal strain tensor related to the displacement field $\boldsymbol{u}$ by $\boldsymbol{\varepsilon} = \nabla^s(\boldsymbol{u})$, $\nabla^s(\bullet)$ being the symmetric gradient of $(\bullet)$, while d is the phase-field parameter taking values between 0 (sound material) and 1 (broken material). Also, the stored elastic energy density $\psi_{el}\left(\boldsymbol{\varepsilon}(\boldsymbol{u}), d\right) = g(d)\psi_0^+\left(\boldsymbol{\varepsilon}(\boldsymbol{u})\right) + \psi_0^-\left(\boldsymbol{\varepsilon}(\boldsymbol{u})\right)$ features the monotonically decreasing *degradation function* $g(d)$ governing the transition from the sound to the cracked state and the decomposition of the undegraded stored energy density ψ_0 into an active part $\psi_0^+\left(\boldsymbol{\varepsilon}(\boldsymbol{u})\right)$ contributing to the crack evolution and an inactive part $\psi_0^-\left(\boldsymbol{\varepsilon}(\boldsymbol{u})\right)$ not participating to the evolution of d [2]. The last term in (1) is the dissipated energy due to fracture, featuring the regularization length ℓ, the fracture toughness G_c the monotonically increasing *dissipation function* $w(d)$ and the normalization constant c_w. Local minimization of the energy (1) under the irreversibility constraint $\dot{d} \geq 0$ leads to the governing equations of the problem in terms of momentum balance and phase-field evolution, along with respective boundary conditions.

The energy (1) allows the crack to evolve only under monotonic loading conditions, making its application unfeasible in case of fatigue loading [3]. To overcome this issue we propose to modify the total energy as [3]

$$E_\ell\left(\boldsymbol{u}, d \,|\, \bar{\alpha}\right) = \int_\Omega \psi_{el}\left(\boldsymbol{\varepsilon}(\boldsymbol{u}), d\right) d\boldsymbol{x} + \\ + \int_\Omega \int_0^t f(\bar{\alpha}(\tau)) \frac{G_c}{4c_w} \left(\frac{w(d)}{\ell} \dot{d} + 2\ell \nabla d \cdot \nabla \dot{d} \right) d\tau d\boldsymbol{x} \,, \tag{2}$$

The introduction of the time integral in (2) makes the energy (time-)history-dependent, therefore we minimize here the rate of the free energy while considering $\bar{\alpha}(t)$ a parameter, namely we freeze its value during a given time step within a time discrete setting. Note that this approximation leads to a non-variational approach.

Using numerical experiments we demonstrate that the framework stemming from (2) is able to reproduce the main characteristics of the fatigue behavior [3], however the associated computational effort is very high, especially for high-fidelity (HF) cycle-by-cycle analysis of components in the high-cycle fatigue regime, namely when a number of cycles N above 10^5 has to be simulated. To reduce the computational cost, we propose a cycle-jump acceleration scheme, whereby the HF computation of a certain number of cycles ΔN is skipped by extrapolating selected local state variables using the results obtained from previous cycles.

In this context, we illustrate an adaptive approach able to automatically determine the extension of the jump to be performed [4]. The core idea lies in adopting as local extrapolated quantity the fatigue history variable at the peak load of the cycle N $\bar{\alpha}(\boldsymbol{x}, N)$, while the decision about when and how many cycles to jump is based on the rate of change of a global scalar variable λ. However, it is not possible to identify a single global variable suitable for this purpose during the whole fatigue life of a component [4]; therefore, we subdivide the fatigue life in three stages, stage I before the onset fatigue effects, stage II during localization of the phase-field variable, and stage III during stable crack propagation until failure. The global variable λ is then defined for stages I, II and III as the maximum fatigue history variable $\max_{\boldsymbol{x}\in\Omega}(\bar{\alpha}(\boldsymbol{x}, N))$, the maximum phase-field variable $\max_{\boldsymbol{x}\in\Omega}(d(\boldsymbol{x}, N))$ and the crack length, respectively [4].

The efficiency of the proposed scheme is first demonstrated by comparing HF and accelerated results , highlighting a speed-up of up to three orders of magnitude. Then, different virtual specimens including complex geometries with multiple cracks, branching and merging are studied. Finally, the obtained accuracy and computational cost are compared with those of other available cycle-jump approaches, demonstrating higher speed-ups and better accuracy.

References

[1] Bourdin, B., Francfort, G. a., and Marigo, J. J. (2000). *Numerical experiments in revisited brittle fracture*, J. Mech. Phys. Sol., **48(4)**, 797–826.

[2] Vicentini, F., Zolesi, C., Carrara, P., Maurini, C. and De Lorenzis, L., *On the energy decomposition in variational phase-field models for brittle fracture under multi-axial stress states*, accepted for publication, Intl. J. Frac. (2024).
[3] Carrara, P., Ambati, M., Alessi, R. and De Lorenzis L., *A framework to model the fatigue behavior of brittle materials based on a variational phase-field approach*, Comp. Meth. App. Mech. Eng., **361**, (2020)
[4] Heizmann, J., Carrara, P., Mirzaei, A.M., Ambati, M., and De Lorenzis, L., *An adaptive acceleration scheme for phase-field modeling of fatigue*, In preparation, (2024).

Optimization of Phase-Field Damage Evolution

Winnifried Wollner
(joint work with R. Haller-Dintelmann, A. Hehl, D. Khimin, H. Meinlschmidt, M. Mohammadi, I. Neitzel, N. Simon, T. Wick)

Within this talk, we will address optimization problems governed by time-discrete phase-field damage processes. The presence of an irreversibility of the fracture growth gives rise to a nonsmooth system of equations. To derive optimality conditions we introduce an additional regularization and show that the resulting optimization problem is well-posed. In particular, under suitable assumptions [1], given an intial phase-field $0 \leq \phi^0 \leq 1$, the Euler-Lagrange equations for $i = 1, \dots, n$

$$\begin{aligned} &\Big(g(\phi^i)\mathbb{C}e(u^i), e(v)\Big) - (q^i, v)_{\partial_N\Omega} = 0 \\ (\mathrm{EL}_\gamma) \qquad &\epsilon(\nabla\phi^i, \nabla\psi) - \frac{1}{\epsilon}(1-\phi^i, \psi) \ + (1-\kappa)(\phi^i\mathbb{C}e(u^i) : e(u^i), \psi) \\ &\qquad +\gamma([(\phi^i - \phi^{i-1})^+]^3, \psi) + \eta(\phi^i - \phi^{i-1}, \psi) = 0 \end{aligned}$$

admit a solution $u^i \in W_D^{1,p}$ and $\phi^i \in L^\infty \cap H^1$ for some $p > 2$.

To tackle discretization errors, as well as convergence in the limit of the irreversibility penalty, an improved differentiability result is shown for the time discrete regularized damage process. It is based on a new differentiability result for solutions of elliptic systems with non smooth coefficients [2]. Based on a bootstrapping argument this result implies the additional regularity $u^i \in H^{1+s}$ for some $s > 0$ uniformly with respect to suitable norms of the control variable q. As a consequence, convergence rates with respect to the mesh size of a discretization of optimization problems governed by the linearized Euler-Lagrange equations can be shown [3]. Moreover, these results allow passing to the limit $\gamma \to \infty$ in the regularization for the Euler-Lagrange equations (EL_γ) giving the expected complementarity system [4]

$$\begin{aligned} &\Big(g(\phi^i)\mathbb{C}e(u^i), e(v)\Big) - (q^i, v)_{\Gamma_N} = 0, \\ (\mathrm{EL}) \qquad &\epsilon(\nabla\phi^i, \nabla\psi) - \frac{1}{\epsilon}(1-\phi^i, \psi) + \eta(\phi^i - \phi^{i-1}, \psi) \\ &\qquad +(1-\kappa)(\phi^i\mathbb{C}e(u^i) : e(u^i), \psi) + (\lambda^i, \psi) = 0, \\ &\qquad \phi^i \leq \phi^{i-1}, \quad \lambda^i \geq 0, \quad (\lambda^i, \phi^i - \phi^{i-1}) = 0. \end{aligned}$$

Moreover, it could be shown, that certain, isolated local, minimizers of the optimization problem

$$\min_{q,u} J(q,u) \qquad \text{s.t. (EL)}$$

can be approximated by local minimizers of

$$\min_{q,u} J(q,u) \qquad \text{s.t. (EL}_\gamma\text{)}.$$

Additionally, convergence of the corresponding first order optimality conditions can be asserted see [5].

Moving away, from control by boundary forces, a coefficient control problem for the obstacle problem

$$\begin{aligned} &\min J(q_\gamma, u_\gamma) \\ &\text{s.t.} \begin{cases} -\nabla \cdot (q_\gamma \nabla u_\gamma) + r(\gamma; u_\gamma) = f & \in L^2(\Omega), \\ u_\gamma \in U, \quad q_\gamma \in Q^{\text{ad}}, \end{cases} \end{aligned}$$

where $r(\gamma; u_\gamma)$ is a smooth regularization of the obstacle $u(x) \leq \psi$, is discussed. For this existence of solutions can be obtained by H-convergence and limiting optimality conditions ($\gamma \to \infty$) can be obtained [6, 7]

References

[1] I. Neitzel, T. Wick, W. Wollner, *An Optimal Control Problem Governed by a Regularized Phase-Field Fracture Propagation Model*, SIAM J. Control Optim. **55** (2017), 2271–2288.

[2] R. Haller-Dintelmann, H. Meinlschmidt, W. Wollner, *Higher regularity for solutions to elliptic systems in divergence form subject to mixed boundary conditions*, Ann. Mat. Pura Appl. **4** (2019), 1227–1241

[3] M. Mohammadi, W. Wollner, *A Priori Error Estimates for a Linearized Fracture Control Problem*, Optim. Eng. **22** (2021), 2127–2149

[4] I. Neitzel, T. Wick, W. Wollner, *An Optimal Control Problem Governed by a Regularized Phase-Field Fracture Propagation Model. Part II The Regularization Limit*, SIAM J. Control Optim. **57** (2019), 1672–1690.

[5] A. Hehl, M. Mohammadi, I. Neitzel, W. Wollner, *Optimizing Fracture Propagation Using a Phase-Field Approach* in Non-Smooth and Complementarity-Based Distributed Parameter Systems, Vol 172 Birkhäuser International Series of Numerical Mathematics (2022), 329–351

[6] N. Simon, W. Wollner, *First Order Limiting Optimality Conditions in the Coefficient Control of an Obstacle Problem* PAMM **22** (2023)

[7] A. Hehl, D. Khimin, I. Neitzel, N. Simon, T. Wick, W. Wollner, *Coefficient Control of Variational Inequalities* arXiv: 2307.00869 (2023)

Phase-field modelling of fatigue fracture in anisotropic aluminium sheets

Martha Kalina (PhD student talk)

We model the cyclic crack propagation under fatigue loading, which is a typical scenario for e. g. fuselage shells of aircrafts due to repetitive take-off and landing. The phase-field method is a promising approach to model arbitrary fracture phenomena like this one. However, fatigue comes along with high numbers of load

cycles, so an explicit simulation of the load path is very expensive. Therefore, time-efficient simulation methods are required. In this contribution, we approach this challenge by combining the phase-field method for brittle fracture with the Local Strain Approach (LSA), an empirical method originally designed for life span estimation of metallic components. In this way, we avoid the explicit simulation of the load cycles by executing a local cyclic damage accumulation. Based on that, the critical fracture energy is degraded locally in order to describe the dissipation due to damage. Metal sheets, such as the aluminium sheet material we consider here, show a distinct anisotropy due to the rolling process during production. Therefore, we now want to take the direction-dependency of fracture into account. Experiments show that from all material parameters it is mainly the fracture toughness which depends on the angle to the sheet's rolling direction. This anisotropy is included in the approximation of the crack surface density.

Reporter: Nicole Buczkowski

Participants

Prof. Dr. Burak Aksoylu
Department of Mathematical, Physical, and Engineering Sciences
Texas A&M University-San Antonio
San Antonio, TX 78224
UNITED STATES

Dr. José C. Bellido
Universidad de Castilla - La Mancha
Departamento de Matemáticas
13071 Ciudad Real
SPAIN

Dr. Debdeep Bhattacharya
Department of Mathematics
The University of Utah
Salt Lake City, UT 84112
UNITED STATES

Prof. Dr. Florin Bobaru
Department of Mechanical and Materials Engineering
University of Nebraska - Lincoln
Lincoln, NE 68588-0526
UNITED STATES

Samira Boddin
FB 10 - Mathematik und Naturwissenschaften
Institut für Mathematik
Universität Kassel
Heinrich-Plett-Straße 40
34132 Kassel
GERMANY

Dr. Nicole Buczkowski
Department of Mathematical Sciences
Worcester Polytechnic Institute
100 Institute Road
Worcester, MA 01609
UNITED STATES

Dr. Pietro Carrara
D-MAVT - Computational Mechanics Group
ETH-Zürich
CLA J17.1
Tannennstr. 3
8092 Zürich
SWITZERLAND

Dr. Fatih Celiker
Department of Mathematics
Wayne State University
656 West Kirby Avenue
Detroit, MI 48202
UNITED STATES

Prof. Dr. Gianni Dal Maso
SISSA
Via Bonomea 265
34136 Trieste
ITALY

Davood Darmicheli
Department of Mathematics
Louisiana State University
Baton Rouge, LA 70803-4918
UNITED STATES

Prof. Dr. Kaushik Dayal
Carnegie Mellon University
College of Engineering
Pittsburgh, PA 15213-3890
UNITED STATES

Prof. Dr. Laura De Lorenzis
CLA J 13
Department of Mechanical and Process Engineering
ETH Zürich
Tannenstr. 3
8092 Zürich
SWITZERLAND

Dr. Patrick Diehl
Department of Physics and Astronomy
Center of Computation and Technology
Louisiana State University
Baton Rouge, LA 70803-4918
UNITED STATES

Prof. Dr. John Dolbow
Department of Mechanical
Engineering
Duke University
P.O. Box Box 90827
Durham, NC 27708-0287
UNITED STATES

Dr. Mikil Foss
Department of Mathematics
University of Nebraska, Lincoln
Lincoln, NE 68588
UNITED STATES

Dr. Francesco Freddi
Dipartimento di Matematica
Universita degli Studi di Parma
Parco Area delle Scienze, 53/A
43124 Parma
ITALY

Alexander Hermann
Helmholtz Center Geesthacht
Max-Planck-Straße 1
21502 Geesthacht
GERMANY

Dr. Francois Hild
Laboratoire de Mécanique Paris-Saclay
(LMPS)
ENS Paris-Saclay
4, avenue des Sciences
91190 Gif-sur-Yvette
FRANCE

Dr. Prashant K. Jha
School of Mechanical and Design
Engineering
University of Portsmouth
Portsmouth PO1 2UP
UNITED KINGDOM

Martha Kalina
TU Dresden
Professur für Numerische und
Experimentelle Festkörpermechanik
Technische Universität Dresden
01062 Dresden
GERMANY

Denis Khimin
Institut für Angewandte Mathematik
Leibniz Universität Hannover
Welfengarten 1
30167 Hannover
GERMANY

Prof. Dr. Dorothee Knees
FB 10 - Mathematik und
Naturwissenschaften
Institut für Mathematik
Universität Kassel
Heinrich-Plett-Straße 40
34132 Kassel
GERMANY

Leon Maximilian Kolditz
Institut für Angewandte Mathematik
Leibniz Universität Hannover
Welfengarten 1
30167 Hannover
GERMANY

Viktor Kosin
Institut für Angewandte Mathematik
Leibniz Universität Hannover
Welfengarten 1
30167 Hannover
GERMANY

Prof. Dr. Giovanni Lancioni
Universita Politecnica delle Marche
via Brecce Bianche, Monte D'Ago
60131 Ancona
ITALY

Prof. Dr. Christopher J. Larsen
Department of Mathematics
Worcester Polytechnic Institute
100 Institute Road
Worcester MA, 01609
UNITED STATES

Prof. Dr. Robert Lipton
Department of Mathematics
Louisiana State University
Baton Rouge LA 70803-4918
UNITED STATES

Prof. Dr. Oscar Lopez-Pamies
Department of Civil and Environmental Engineering,
University of Illinois at Urbana Champaign
3106 Newmark Lab, 205 North Mathews Ave.
Urbana, IL 61822
UNITED STATES

Prof. Dr. Corrado Maurini
Sorbonne Université
Institut Jean Le Rond d'Alembert (UMR 7190)
4 Place Jussieu
75252 Paris Cedex 5
FRANCE

Dr. Boris Muha
Department of Mathematics
University of Zagreb
Bijenicka 30
10000 Zagreb
CROATIA

Prof. Dr. Matteo Negri
Dipartimento di Matematica
Università di Pavia
Via Ferrata, 5
27100 Pavia
ITALY

Prof. Dr. Ira Neitzel
Institut für Numerische Simulation
Universität Bonn
Friedrich Hirzebruch Allee 7
53115 Bonn
GERMANY

Dr. Greta Ongaro
Department of Structural and Geotechnical Engineering
Sapienza University of Rome
Via Eudossiana 18
00184 Roma
ITALY

Prof. Dr. Anna Pandolfi
Civil and Environmental Engineering Department
Politecnico di Milano
Piazza Leonardo da Vinci, 32
20133 Milano
ITALY

Kai Partmann
Lehrstuhl für Festkörpermechanik
Department Maschinenbau, Fakultät IV
Universität Siegen
Paul-Bonatz-Str.
Postfach 9-11
57076 Siegen
GERMANY

Dr. Maryam Parvizi
Institut für Angewandte Mathematik
Leibniz Universität Hannover
Welfengarten 1
30167 Hannover
GERMANY

Anna Pernatii
Fakultät für Mathematik
Otto-von-Guericke-Universität
Magdeburg
Postfach 4120
39016 Magdeburg
GERMANY

Prof. Dr. Serge Prudhomme
Polytechnique Montreal
Case Postale 6079
Montréal QC H3C 3A7
CANADA

Prof. Dr. Petronela Radu
Department of Mathematics
University of Nebraska, Lincoln
Lincoln NE 68588
UNITED STATES

Dr. Davide Riccobelli
Dipartimento di Matematica
Politecnico di Milano
Via Bonardi 9
20133 Milano
ITALY

Prof. Dr. Tomáš Roubíček
Mathematical Institute
Charles University
Sokolovska 83
186 75 Praha 8
CZECH REPUBLIC

Nuwanthi Samarawickrama
Department of Mathematics
Louisiana State University
Baton Rouge, LA 70803-4918
UNITED STATES

Prof. Dr. Oliver Sander
Institut für Numerische Mathematik
Technische Universität Dresden
Zellescher Weg 12-14
01069 Dresden
GERMANY

Prof. Dr. Bernd Schmidt
Institut für Mathematik
Universität Augsburg
86135 Augsburg
GERMANY

Prof. Dr. Marc Alexander Schweitzer
Institut für Numerische Simulation
Universität Bonn
und
Fraunhofer SCAI
Friedrich-Hirzebruch-Allee 7
53115 Bonn
GERMANY

Dr. James Scott
Department of Applied Physics and Applied Mathematics, Columbia University
New York New York, 10027
UNITED STATES

Dr. Pablo Seleson
Oak Ridge National Laboratory
P.O. Box 2008
Oak Ridge 37831
UNITED STATES

Dr. Arman Shojaei
Helmholtz Center Geesthacht
Max-Planck-Straße 1
21502 Geesthacht
GERMANY

Prof. Dr. Marita Thomas
Freie Universität Berlin und
Weierstraß-Institut für Angewandte Analysis und Stochastik
Arnimallee 9
14195 Berlin
GERMANY

Dr. Rodica Toader
Dip. di Matematica e Informatica
Universita di Trieste
Via Alfonso Valerio 12/1
34127 Trieste
ITALY

Dr. Nathaniel Trask
Applied Mathematics Division
Sandia National Laboratories
Albuquerque 87185
UNITED STATES

Prof. Dr. Lev Truskinovsky
Physique et Mecanique des Milieux Heterogenes
CNRS - UMR 7636
ESPCI ParisTech
10 Rue Vauquelin
75005 Paris
FRANCE

Dr. Henry von Wahl
Mathematisches Institut
Universität Jena
Ernst-Abbe-Platz 2-4
07743 Jena
GERMANY

Ana Vrgoc
Laboratory of Experimental Mechanics, Faculty of Mechanical Engineering and Naval Architecture
University of Zagreb
Ivana Lucica 5
10002 Zagreb
CROATIA

Prof. Dr. Kerstin Weinberg
Fachbereich 11 / Maschinentechnik
Institut für Mechanik und Regelungstechnik
Universität Siegen
Paul-Bonatz-Straße 9 - 11
57068 Siegen
GERMANY

Prof. Dr. Thomas Wick
Institut für Angewandte Mathematik
Leibniz Universität Hannover
Welfengarten 1
30167 Hannover
GERMANY

Prof. Dr. Christian Wieners
Fakultät für Mathematik
Institut für Angewandte und Numerische Mathematik
Karlsruher Institut für Technologie (KIT)
Englerstraße 2
76131 Karlsruhe
GERMANY

Prof. Dr. Winnifried Wollner
Fachbereich Mathematik
Universität Hamburg
Bundesstr. 55
20146 Hamburg
GERMANY

Prof. Dr. Rena C. Yu
Universidad de Castilla-La Mancha
Departamento de Mecánica Aplicada e Ingeniería de Proyectos
ETSI de Caminos, Canales y Puertos
Avda. Camilo José Cela
13071 Ciudad Real 13071
SPAIN

Prof. Dr. Yue Yu
Department of Mathematics
Lehigh University
14 E. Packer Avenue
Bethlehem, PA 18015-1237
UNITED STATES